arXiv:hep-ph/0007050v1 5 Jul 2000

McGILL-00-03
UA/NPPS-04-00

Next-to-Leading Order Corrections to Heavy Flavour Production in Longitudinally Polarized Photon-Nucleon Collisions

Z. Merebashvili^{a,*,1}, A.P. Contogouris^{a,b,2} and G. Grispos^{b,3}

a. Department of Physics, McGill University, Montreal, Qc., H3A 2T8, Canada

b. Nuclear and Particle Physics, University of Athens, Athens 15771, Greece

ABSTRACT

A complete next-to-leading order calculation of longitudinally polarized heavy quark photoproduction is presented. All results of the purturbative calculation are given in detail. For reactions and energies of interest cross sections differential in the transverse momentum and rapidity of the heavy quark, total cross sections and the corresponding asymmetries are given. Errors in the asymmetries are estimated and the possibility to distinguish between various scerarios of the polarized gluon distribution is discussed. Our results are compared with other related publications.

---

[*] Present address: High Energy Physics Institute, Tbilisi State University, University St. 9, 380086 Tbilisi, Republic of Georgia.

[1] e-mail: mereb@sun20.hepi.edu.ge

[2] e-mail: apcont@physics.mcgill.ca, acontog@cc.uoa.gr

[3] e-mail: ggrispos@cc.uoa.gr

I. INTRODUCTION

Deep inelastic scattering of longitudinally polarized particles has provided important information on the spin structure of the nucleon. However, the size and shape of the polarized gluon distribution Δg in the proton remains an essential problem. Significant progress requires experiments on reactions with longitudinally polarized particles dominated by subprocesses with initial gluons. Such a reaction is

$$\vec{\gamma} + \vec{p} \rightarrow Q(\bar{Q}) + X, \tag{1.1}$$

where $Q(\bar{Q})$ denotes heavy quark (antiquark); this is dominated by

$$\vec{\gamma} + \vec{g} \rightarrow Q + \bar{Q} \tag{1.2}$$

An experiment closely related to (1.1) is soon going to take place [1] and there are more than one proposals [2].

At the Born level, (1.1) has been studied long ago [3,4]. However, the importance of knowing the next-to-leading order corrections (NLOC) cannot be overemphasized. This work presents detailed results on a NLOC calculation.

It should be noted that NLOC for (1.1) have already been published [5]. We believe, however, that in view of the importance of (1.1), an independent determination of NLOC in a different regularization approach (see below) is in order. Extensive comparisons with the calculation of [5], as well as certain differences in our view regarding certain questions will be also reported.

At NLO, apart from the loop and gluon Bremsstrahlung (Brems) contributions to (1.2), the subprocesses

$$\vec{\gamma} + \vec{q}(\vec{\bar{q}}) \rightarrow Q + \bar{Q} + q(\bar{q}), \tag{1.3}$$

where q denotes a light quark, should also be taken into account.

We note that the Abelian part of NLOC for (1.4) provides the corrections to

$$\vec{\gamma} + \vec{\gamma} \rightarrow Q + \bar{Q} \tag{1.4}$$

This part has already been determined [6,7]. NLOC to (1.4) are of interest in themselves in connection with Higgs boson searches when the Higgs mass is in the range of 90 to 160 GeV.

The loop and 2 → 3 parton graphs involved in NLOC introduce ultraviolet (UV), infrared (IR) and collinear singularities, which are eliminated by working in $n = 4 - 2\varepsilon$ dimensions. For polarized reactions this requires extension of the Dirac matrix γ_5 in $n \neq 4$ dimensions. Unless otherwise stated, we work in the scheme of dimensional reduction (RD), which simplifies the calculation of the traces. Certain subtleties of RD have been discussed in [6] and are mentioned below. Furthermore, we use parton distributions whose evolution, via 2-loop anomalous dimensions, is determined in a scheme different from RD. This necessitates the addition to our perturbative results of certain conversion terms.

In all the above contributions the photon interacts in a direct way. In addition, there are also resolved contributions, in which it interacts through its partonic constituents; in fact, strictly speaking, at NLO, scheme independent cross sections arise only by adding them. At this moment a complete calculation of the resolved contributions is not possible, and we will be limited in giving an estimate.

The paper is organized as follows. Sect. II contains our general procedures, Sect. III discusses the loop contributions to the photon-gluon fusion subprocess and Sect. IV the corresponding Brems ones. Sect. V presents analytic results on the subprocess (1.3). In Sect. VI we derive the nesessary formulas for calculating various physical observables. Sect. VII presents our numerical results and discusses the possibility to distinguish between three sets differing essentially in the polarized gluon distribution function Δg. Sect. VIII deals with our comparison with [5], as well as with [8]. Sect. IX presents our conclusions. Finally, in three Appendices we present results completing our determination of NLOC.

II. GENERAL PROCEDURES

The Born and the loop contributions to $\gamma + g \to Q + \bar{Q}$ are shown in Fig. 1. With the 4-momenta $p_i, i = 1, ..., 4$, as indicated and with m the heavy quark mass we define:

$$s \equiv (p_1 + p_2)^2, \qquad t \equiv T - m^2 \equiv (p_1 - p_3)^2 - m^2, \qquad u \equiv U - m^2 \equiv (p_2 - p_3)^2 - m^2 \quad (2.1)$$

Let $M_i(\lambda_1, \lambda_2)$ the amplitude of any of the contributing graphs, where λ_1, λ_2 the helicities of the initial partons; our polarized cross sections correspond to the quantities:

$$\frac{1}{2}\Sigma[M_i(++) \overset{*}{M}_j (++) - M_i(+-) \overset{*}{M}_j (+-)] \qquad (2.2)$$

where Σ denotes summation over the helicities and colors of the final particles and average over the colors of the initial. For the determination of the asymmetries we need also the unpolarized cross sections, which correspond to the average of $M_i(++) \overset{*}{M}_j (++)$ and $M_i(+-) \overset{*}{M}_j (+-)$.

We also introduce

$$v \equiv 1 + t/s \qquad\qquad w \equiv -u/(s + t) \qquad (2.3)$$

To reduce the length of the subsequent expressions we will make use of the results presented in [6]. Thus our leading-order (LO) polarized and unpolarized cross sections are

$$[\Delta]\frac{d\sigma_{\rm LO}^{\gamma g}}{dvdw} = \kappa C_F [\Delta]\frac{d\sigma_{\rm LO}}{dvdw} \qquad (2.4)$$

where $\kappa \equiv \alpha_s/8\alpha e_Q^2$ and $[\Delta]d\sigma_{\rm LO}/dvdw$ the corresponding [polarized] unpolarized cross sections for $\gamma\gamma \to Q\bar{Q}$ (Eq. (9) of [6]). For later use we note that $[\Delta]d\sigma_{\rm LO}/dvdw$ are proportional to:

$$\Delta B(s, t, u) = \frac{1}{s}\left(-\frac{t^2 + u^2}{tu} + 2\frac{sm^2}{tu}\left(\frac{s^2}{tu} - 2\right)\right)$$

and (see also [8])

$$B(s,t,u) = \frac{1}{s}\left(\frac{t^2+u^2}{tu} + 4\frac{sm^2}{tu}\left(1-\frac{sm^2}{tu}\right)\right) \tag{2.5}$$

In determining the loop contributions, the renormalization of the heavy quark mass and wave function were carried on shell, as in [6], i.e. the renormalized heavy quark self-energy $\Sigma_r(p)$ was taken to satisfy at $p^2 = m^2$:

$$\Sigma_r(p) = 0 \qquad\qquad \frac{\partial}{\partial p}\Sigma_r(p) = 0 \tag{2.6}$$

This determines the mass and wave function renormalization constants Z_m and Z_2 [6].

Dimensional reduction does not automatically satisfy the Ward identity

$$Z_1 = Z_2,$$

where Z_1 is the renormalization constant for the vertex of the graph Fig. 1(d). This requires the introduction of proper finite counterterm, of which the form is given in [6].

In the present case charge renormalization is also required. Defining

$$C_\varepsilon(m) \equiv \frac{\Gamma(1+\varepsilon)}{(4\pi)^2}\left(\frac{4\pi\mu^2}{m^2}\right)^\varepsilon, \tag{2.7}$$

let $g_0(g)$ be the bare (renormalized) coupling, $Z_g = g_0/g$ the charge renormalization constant and $b = (11N_C - 2N_{lf})/6$, where N_{lf} is the number of light flavors. We take

$$Z_g = 1 - \frac{g^2}{\varepsilon}\left\{C_\varepsilon(M)b - \frac{1}{3}C_\varepsilon(m)\right\} \tag{2.8}$$

where M is a regularization mass. In this scheme the contribution of a heavy quark loop in the gluon self-energy is subtracted out, i.e. the heavy quark is decoupled [9,8]. This is consistent with parton distributions $\Delta F_{a/p}(x,Q^2)$ of which the evolution is determined from split functions involving only light quarks, as is the case of $\Delta F_{a/p}$ used below.

Finally, the renormalization of the $gQ\bar{Q}$ vertex was carried using the Slavnov-Taylor identities [10].

III. LOOP CONTRIBUTIONS

The loop graphs contributing to (1.2) are depicted in Fig. 1. The integrals for the Abelian type of graphs (a)-(e) were calculated in [6]. The non-Abelian graphs (g) and (h) introduce tensor integrals of the form

$$\int \frac{d^nq}{(2\pi)^n}\frac{q^\mu, q^\mu q^\nu}{q^2(q-p_2)^2[(q+p_4-p_2)^2-m^2]}$$

and

$$\int \frac{d^n q}{(2\pi)^n} \frac{q^\mu, q^\mu q^\nu, q^\mu q^\nu q^\rho}{q^2 (q-p_2)^2 [(q+p_4-p_2)^2 - m^2][(q-p_3)^2 - m^2]}$$

As in [6], using Passarino-Veltman techniques [11], we reduce them to scalar ones; those can be found in [12].

The contributions presented below include the $t \leftrightarrow u$ crossing symmetric of Fig. 1 plus UV counterterms; thus they contain no UV singularities.

The graphs (a)-(e) give:

$$\frac{d\sigma^{\gamma g}_{a-e}}{dv dw} = \kappa C_F \frac{d\sigma_{\rm vse}}{dv dw} - \frac{N_C}{2} \frac{d\sigma_{a-e}}{dv} \delta(1-w) \tag{3.1}$$

where $d\sigma_{\rm vse}/dvdw$ is given in Eq.(16) of [6] and

$$\begin{aligned} \frac{d\sigma_{a-e}}{dv} &= K_L \{ 2\tilde{A}_1 [2(\zeta(2) - {\rm Li}_2(\frac{T}{m^2}))(1 + 3\frac{m^2}{t}) - \ln(\frac{-t}{m^2})(1 + \frac{m^2}{T}) + 2] + \tilde{A}_2 \ln(\frac{-t}{m^2}) \\ & \quad + \tilde{A}_3 ({\rm Li}_2(\frac{T}{m^2}) - \zeta(2)) + \tilde{A}_4 + (t \leftrightarrow u) \} \end{aligned} \tag{3.2}$$

with

$$K_L \equiv \frac{1}{8s} \alpha \alpha_s^2 e_Q^2$$

Here and subsequently the polarized cross sections are given by (3.1) and (3.2) with $\Delta d\sigma/dvdw$, $\Delta d\sigma/dv$ and $\Delta\tilde{A}_1$, i=1,...,4, replacing the corresponding unpolarized quantities. The $[\Delta]\tilde{A}_i$ are given in Appendix A.

Graph (f) contributes:

$$\frac{d\sigma_f}{dv dw} = \kappa (C_F - \frac{N_C}{2}) \frac{d\sigma_{\rm box}}{dv dw} \tag{3.3}$$

with $d\sigma_{\rm box}/dvdw$ in Eq.(22) of [6].

Turning to the non-Abelian graphs, (g) gives

$$\frac{d\sigma^{\gamma g}_{g}}{dv dw} = -2\pi \alpha_s C_\varepsilon(m) N_C \frac{d\sigma^{\gamma g}_{\rm LO}}{dv dw} \left(\frac{1}{\varepsilon^2} + \frac{4}{\varepsilon} \right) - \frac{N_C}{2} \left(\frac{d\tilde{\sigma}_g}{dv} + \frac{d\sigma_g}{dv} \right) \delta(1-w), \tag{3.4}$$

where

$$\frac{d\tilde{\sigma}_g}{dv} = 2F(\varepsilon) \left\{ -A_1 \frac{1}{\varepsilon} \ln(\frac{-t}{m^2}) + A'_1 \left[\frac{1}{\varepsilon^2} - \frac{2}{\varepsilon} - \frac{2}{\varepsilon} \ln(\frac{-t}{m^2}) \right] + (t \leftrightarrow u) \right\} \tag{3.5}$$

with

$$F(\varepsilon) \equiv K_L \mu^{2\varepsilon} \left(\frac{4\pi\mu}{m} \right)^{2\varepsilon} \frac{\Gamma(1+\varepsilon)}{\Gamma(1-\varepsilon)} \left(\frac{s\mu^2}{tu - sm^2} \right)^{\varepsilon} \tag{3.6}$$

and

$$\begin{aligned} \frac{d\sigma_g}{dv} = K_L \{ & 2A_1 [{\rm Li}_2(\frac{T}{m^2}) + \ln^2(\frac{-t}{m^2}) - 2] + A'_1 [4{\rm Li}_2(\frac{T}{m^2}) + 4\ln^2(\frac{-t}{m^2})] \\ & + A'_2 \ln(\frac{-t}{m^2}) + A'_3 + (t \leftrightarrow u) \} \end{aligned} \tag{3.7}$$

In (3.5) and (3.7), $[\Delta]A_1$ are given in App. B of [6] and $[\Delta]A'_i$, i=1,2,3, in App. A of this paper.

The contribution of the graph (h) is:

$$\frac{d\sigma_h^{\gamma g}}{dvdw} = -\frac{N_C}{2}\left\{4\pi\alpha_s C_\varepsilon(m)\frac{3}{\varepsilon^2}\frac{d\sigma_{\rm LO}^{\gamma g}}{dvdw} + \left(\frac{d\tilde{\sigma}_h}{dv} + \frac{d\sigma_h}{dv}\right)\delta(1-w)\right\}, \tag{3.8}$$

where

$$\frac{d\tilde{\sigma}_h}{dv} = 2F(\varepsilon)\left\{-A_1\frac{1}{\varepsilon}\left[\ln(\frac{-t}{m^2}) + 2\ln(\frac{-u}{m^2})\right] + A'_1\left[-\frac{1}{\varepsilon^2} + \frac{2}{\varepsilon} + \frac{2}{\varepsilon}\ln(\frac{-t}{m^2})\right] + (t \leftrightarrow u)\right\} \tag{3.9}$$

and

$$\begin{aligned}\frac{d\sigma_h}{dv} = K_L\{&A_1[-\frac{35}{4}\zeta(2) - {\rm Li}_2(\frac{T}{m^2}) + 4\ln(\frac{-t}{m^2})\ln(\frac{-u}{m^2}) - \ln^2(\frac{-t}{m^2})] + B'_1{\rm Li}_2(\frac{T}{m^2})\\ &+(B'_2 + A'_1)\zeta(2) + B'_3\ln^2(\frac{-t}{m^2}) + B'_4\ln(\frac{-t}{m^2}) + B'_5\ln(\frac{-t}{m^2})\ln(\frac{-u}{m^2})\\ &+B'_6 + (t \leftrightarrow u)\}\end{aligned} \tag{3.10}$$

The coefficients $[\Delta]B'_i$, i=1,...,6, are given in App. A.

Finally, after cancellation of the UV singularities, graph (i) does not contribute.

We remark that regarding the terms $1/\varepsilon^2$, the contributions of the graphs (g) and (h) taken separately are not proportional to the Born $d\sigma_{\rm LO}^{\gamma g}/dvdw$; only their sum is proportional to the Born. The same holds regarding the terms $1/\varepsilon$.

IV. GLUON BREMS CONTRIBUTIONS

In this chapter we present complete analytic results for the NLOC arising from Brems. To the best of our knowledge, in relation with heavy quark production, such results have not so far been presented.

With k the 4-momentum of the emitted gluon we introduce also

$$s_2 \equiv (k + p_4)^2 - m^2 = s + t + u = sv(1-w) \tag{4.1}$$

The Brems graphs contributing to the NLOC of (1.2) are shown in Fig. 2A. The squared sum of the corresponding amplitudes (plus those obtained via $p_1 \leftrightarrow p_2$) after summing over final spins and colors and averaging over initial colors is given by

$$4m^2|M_{2\leftrightarrow 3}^{\gamma g}|^2 = K_B(\varepsilon)\left(\frac{C_F}{2}G^{\gamma\gamma} - \frac{N_C}{16}G^{\gamma g}\right) \tag{4.2}$$

where $G^{\gamma\gamma}$ is the quantity in the square bracket of Eq.(24) of [6] (plus $p_1 \leftrightarrow p_2$), $G^{\gamma g}$ has the expansion

$$\begin{aligned}
G^{\gamma g} &= e_1 + \frac{e_2}{p_2\cdot p_4} + \frac{e_3}{p_1\cdot p_4^2} + \frac{e_4}{p_1\cdot p_4} + \frac{\tilde{e}_5}{p_3\cdot k} + \frac{\tilde{e}_6}{p_1\cdot p_4\ p_3\cdot k} + \frac{e_7}{p_1\cdot p_4\ p_2\cdot p_4} + e_8\frac{p_2\cdot k}{p_1\cdot p_4} \\
&+ \frac{\tilde{e}_9}{p_2\cdot p_4\ p_3\cdot k} + e_{10}\frac{p_2\cdot k}{p_3\cdot k} + \frac{e_{11}}{p_1\cdot p_4^2\ p_3\cdot k} + f_1\frac{p_3\cdot k}{p_2\cdot p_4} + f_2\frac{p_3\cdot k^{\,2}}{p_2\cdot p_4} + \tilde{f}_3\frac{p_3\cdot k^{\,2}}{p_2\cdot k} + \tilde{f}_4\frac{p_3\cdot k}{p_2\cdot k} \\
&+ \frac{\tilde{f}_5}{p_2\cdot k} + \frac{\tilde{f}_6}{p_1\cdot p_4\ p_2\cdot k} + \frac{\tilde{f}_7}{p_2\cdot k^{\,2}} + \frac{\tilde{f}_8}{p_1\cdot p_4\ p_2\cdot k^{\,2}} + \frac{\tilde{f}_9}{p_2\cdot k\ p_3\cdot k} + \frac{\tilde{f}_{10}}{p_1\cdot p_4^2\ p_2\cdot k} \\
&+ \frac{\tilde{f}_{11}}{p_1\cdot p_4^2\ p_2\cdot k^{\,2}} \qquad (4.3)
\end{aligned}$$

and

$$K_B(\varepsilon) = (4\pi)^3\alpha\alpha_s^2 e_Q^2\mu^{6\varepsilon} \qquad (4.4)$$

As in Sect. III, $\Delta|M_{2\to 3}^{\gamma g}|^2$ is given by (4.2) and (4.3) with $\Delta G^{\gamma\gamma}$, $\Delta G^{\gamma g}$, Δe_i and Δf_i, i=1,2,...,13, replacing the corresponding unpolarized quantities. The coefficients $[\Delta]e_i$, $[\Delta]f_i$ of (4.3) are given in App. B.

The Brems contribution to $[\Delta]d\sigma/dvdw$ is obtained by working in the Gottfried-Jackson frame of $\bar{Q}(Q)$ and gluon (c.m. system of p_4 and k). Details are given in [6]. The terms with coefficients $[\Delta]\tilde{e}_i$, $[\Delta]\tilde{f}_i$ in (4.3) give contributions singular at $s_2 = 0$ ($w = 1$) and must be integrated in $n \neq 4$ dimensions. In view of the fact that the $2 \to 3$ particle phase space is proportional to $s_2^{1-2\varepsilon}$ (Eq. (26) of [6]), the remaining terms can be integrated in 4 dimensions. The arising integrals are given in [12]. Certain terms of special interest not given in [6] are determined in App. C.

Corresponding to the second term in (4.2), with $\bar{y} \equiv \sqrt{(t+u)^2 - 4m^2 s}$, $S_2 = s_2 + m^2$ and $x = (1-\beta)/(1+\beta)$, where $\beta = \sqrt{1 - 4m^2/s}$, the final result is

$$\begin{aligned}
\frac{d\sigma_{\mathrm{Br}}^{\gamma g}}{dvdw} &= -\frac{K_B(0)}{(4\pi)^3}\frac{N_C}{16}2\pi\frac{vs_2}{8\pi S_2}\{e_1 + \frac{2S_2}{s_2(s+u)}\ln\frac{S_2}{m^2}\ e_2 + \frac{4S_2}{m^2(s+t)^2}e_3 + \frac{2S_2}{s_2(s+t)}\ln\frac{S_2}{m^2}\ e_4 \\
&+ e_7 I_8 + e_8 I_{10} + e_{10} I_{16} + e_{11} I_{13}(t \leftrightarrow u) + f_1 F_1 + f_2 F_2\} \\
&- \frac{1}{(1-w)_+}\frac{s_2^2}{S_2}\frac{N_C}{16}F(0)\{\frac{2S_2}{s_2\bar{y}}\ln\frac{T+U-\bar{y}}{T+U+\bar{y}}\ \tilde{e}_5 + \tilde{e}_6 I_{11}(t \leftrightarrow u) + \tilde{e}_9 I_{11}\} \\
&- \frac{vss_2}{S_2}\frac{N_C}{16}F(0)\{\tilde{f}_3F_3^c + \tilde{f}_4F_4^c + \tilde{f}_7F_7^c + \tilde{f}_8F_8^c + \tilde{f}_{10}F_{10}^c + \tilde{f}_{11}F_{11}^c - (2\ln\frac{s_2}{m^2} + \ln\frac{m^2}{S_2})(\tilde{f}_3F_3^s \\
&+ \tilde{f}_4F_4^s + \tilde{f}_8F_8^s + \tilde{f}_{10}F_{10}^s + \tilde{f}_{11}F_{11}^s)\} \\
&- \frac{1}{(1-w)_+}\frac{s_2^2}{S_2}\frac{N_C}{16}F(0)\{\tilde{f}_6F_6^c + \tilde{f}_9F_9^c - (2\ln\frac{sv}{m^2} + \ln\frac{m^2}{S_2})(\tilde{f}_5F_5^s + \tilde{f}_6F_6^s + \tilde{f}_9F_9^s)\} \\
&+ 2L_+\frac{s_2^2}{S_2}\frac{N_C}{16}F(0)\{\tilde{f}_5F_5^s + \tilde{f}_6F_6^s + \tilde{f}_9F_9^s\}
\end{aligned}$$

$$
\begin{aligned}
&+\;\; 8\pi\alpha_s N_C C_\varepsilon(m)[\Delta]\frac{d\sigma^{\gamma g}_{\mathrm{LO}}}{dvdw}\{2\ln^2\frac{sv}{m^2}-\ln^2(x)+\frac{1}{2}\ln^2(\frac{t}{u}x)+2\ln\frac{u}{t}\ln\frac{sv}{m^2}+\mathrm{Li}_2(1-\frac{1}{x}\frac{u}{t})\\
&-\;\; \mathrm{Li}_2(1-\frac{1}{x}\frac{t}{u})-2\zeta(2)-\frac{2m^2-s}{s\beta}[(2\ln\frac{sv}{m^2}-\ln(x))\ln(x)-\mathrm{Li}_2\left(\frac{-4\beta}{(1-\beta)^2}\right)]]\}
\end{aligned}
\qquad (4.5)
$$

In Eq. (4.5), the integrals I_i are given in the App. C of [6] and the integrals F_i in the App. C of this paper. Also, $L_+ \equiv (\ln(1-w)/(1-w))_+$, which enters through the relation

$$
(1-w)^{-1-2\varepsilon} = -\frac{1}{2\varepsilon}\delta(1-w) + \frac{1}{(1-w)_+} - 2\varepsilon L_+, \qquad (4.6)
$$

where the so called "plus" distributions are defined in a usual way:

$$
\int_0^1 dz\frac{f(w)}{(1-w)_+} \equiv \int_0^1 dz\frac{f(w)-f(1)}{1-w}. \qquad (4.7)
$$

For the second term of (4.2), we give the terms $\sim 1/\varepsilon^2$ and $1/\varepsilon$, as well:

$$
\begin{aligned}
\frac{d\sigma^{\gamma g,\varepsilon}_{\mathrm{Br}}}{dvdw} &= \frac{N_C}{\varepsilon^2}8\pi\alpha_s C_\varepsilon(m)[\Delta]\frac{d\sigma^{\gamma g}_{\mathrm{LO}}}{dvdw} - \frac{N_C}{\varepsilon}8\pi\alpha_s C_\varepsilon(m)[\Delta]\frac{d\sigma^{\gamma g}_{\mathrm{LO}}}{dvdw}\{3\ln(\frac{-u}{m^2})-\ln(\frac{-t}{m^2})\}\\
&+ \frac{N_C}{\varepsilon}8\pi\alpha_s C_\varepsilon(m)[\Delta]\frac{d\sigma^{\gamma g}_{\mathrm{LO}}}{dvdw}\frac{2m^2-s}{s\beta}\ln(x)\\
&- \frac{1}{\varepsilon}\frac{2sv}{1-vw}F(\varepsilon)[\Delta]P^f_{gg}(x_2)[\Delta]B(x_2 s,t,x_2 u)
\end{aligned}
\qquad (4.8)
$$

where $[\Delta]P^f_{gg}(x)$ is the 4-dimensional $g \to gg$ split function without the $\delta(1-w)$ part, $F(\varepsilon)$, $[\Delta]B(s,t,u)$ are given by (3.6) and (2.5) and

$$
x_2 = \frac{1-v}{1-vw} \qquad (4.9)
$$

Addition of loop and Brems contributions cancels the singularities $1/\varepsilon^2$ and part of the $1/\varepsilon$. The remaining $1/\varepsilon$ are cancelled by a factorization counterterm corresponding to the final gluon emitted collinearly with the initial one (Fig. 2A, graph (d)). In the $\overline{MS}$ scheme this counterterm gives:

$$
[\Delta]\frac{d\sigma_{\mathrm{ct}}}{dvdw} = \frac{1}{\varepsilon}\frac{2sv}{1-vw}F(\varepsilon)[\Delta]P_{gg}(x_2)[\Delta]B(x_2 s,t,x_2 u)\left(\frac{m^2}{M_F^2}\right)^{\varepsilon}, \qquad (4.10)
$$

$[\Delta]P_{gg}(x)$ the $g \to gg$ split function and M_F the factorization scale.

Our cross sections will be convoluted with parton distributions evolved via two-loop split functions. In n dimensions the split functions have the form

$$
[\Delta]P^n_{ba}(x,\varepsilon) = [\Delta]P_{ba}(x) + \varepsilon[\Delta]P^\varepsilon_{ba}(x) \qquad (4.11)
$$

The polarized split functions have been determined [13,14] in the t'Hooft-Veltman scheme [15] modified so that $\Delta P^n_{qq}(x,\varepsilon) = P^n_{qq}(x,\varepsilon)$. In this scheme

$$\Delta P^{\varepsilon}_{gg}(x) = 4N_C(1-x) + \frac{1}{6}N_{lf}\delta(1-x) \tag{4.12}$$

However, our calculations were carried in dimensional reduction (Sect. I), where

$$\Delta P^{\varepsilon}_{ab}(x) = P^{\varepsilon}_{ab}(x) = 0 \tag{4.13}$$

Thus, a conversion term $\Delta d\sigma_{\rm conv}/dvdw$ should be added to our $\Delta d\sigma^{\gamma g}/dvdw$. Conversion terms are determined from the difference of $[\Delta]P^{\varepsilon}_{ab}(x)$ in the two schemes [16]: In the present case

$$\Delta\frac{d\sigma_{\rm conv}}{dvdw} = -\frac{2sv}{1-vw}F(0)\Delta P^{\varepsilon}_{gg}(x_2)\Delta B(x_2 s, t, x_2 u) \tag{4.14}$$

with $\Delta P^{\varepsilon}_{gg}(x)$ given by (4.11).

The unpolarized parton distributions we use were evolved in the $\overline{MS}$ scheme, where $P^{\varepsilon}_{gg}(x) = 0$. Thus conversion term is not required.

V. SUBPROCESS $\gamma q \to Q\bar{Q}q$

The graphs contributing to this subprocess are shown in Fig. 2B. The squared sum of the corresponding amplitudes, after summing over spins and colors and averaging over initial colors, is given by

$$4m^2|M^{\gamma q}_{2\to 3}|^2 = \frac{2}{N_C}(4\pi)^3\alpha\alpha_s^2(e_Q^2 Q_1 + e_q^2 Q_2 + e_Q e_q Q_3) \tag{5.1}$$

where e_q the charge of the light quark q. $|M^{\gamma\bar{q}}_{2\to 3}|^2$ corresponding to $\gamma\bar{q} \to Q\bar{Q}\bar{q}$ is given by the same expression with an opposite sign of the last term. The quantity Q_1 is given by an expansion similar to (4.3). Next we introduce

$$s_{34} \equiv p_3\cdot p_4 + m^2 \tag{5.2}$$

Then Q_2 and Q_3 are of the form:

$$\begin{aligned} Q_{2,3} = {} & e_1 + \frac{e_4}{p_1\cdot p_4} + e_8\frac{p_2\cdot k}{p_1\cdot p_4} + \tilde{f}_4\frac{p_3\cdot k}{p_2\cdot k} + \frac{\tilde{f}_5}{p_2\cdot k} + \frac{\tilde{f}_6}{p_1\cdot p_4\; p_2\cdot k} + f_{12}\frac{p_1\cdot k}{s_{34}} + f_{13}\frac{p_1\cdot k}{s_{34}^2} \\ + {} & \frac{f_{14}}{s_{34}} + \frac{\tilde{f}_{15}}{p_1\cdot k} + \frac{\tilde{f}_{16}}{s_{34}\; p_1\cdot k} + \frac{\tilde{f}_{17}}{s_{34}^2\; p_1\cdot k} + \frac{f_{18}}{s_{34}\; p_1\cdot p_4} + \frac{\tilde{f}_{19}}{p_1\cdot k\; p_2\cdot k} + \tilde{f}_{20}\frac{p_3\cdot k}{p_1\cdot k} \\ + {} & \frac{\tilde{f}_{21}}{s_{34}\; p_2\cdot k} \end{aligned} \tag{5.3}$$

As before, $\Delta|M^{\gamma g}_{2\to 3}|^2$ is given by (5.1) and (5.3) with ΔQ_r, r=1,2,3, Δe_i and Δf_j replacing Q_r, e_i and f_j. The coefficients $[\Delta]e_i$ and $[\Delta]f_j$ are given in the last part of App. B.

The contribution to $[\Delta]d\sigma/dvdw$ is obtained by working as in Sect. 4 (c.m. frame of $\bar{Q}(Q)$ and final light quark). Again the terms with coefficients $[\Delta]\tilde{e}_i$ and $[\Delta]\tilde{f}_j$ must be integrated in n dimensions.

After phase space integrations, we get the following results for the sets Q_1, Q_2 and Q_3:

$$\begin{aligned}\frac{d\sigma^{\gamma q,Q_1}_{\rm Br}}{dvdw} &= Le_Q^2\{e_1 + \frac{4S_2}{m^2(s+t)^2}e_3 + \frac{2S_2}{s_2(s+t)}\ln\frac{S_2}{m^2}\ e_4 + e_8 I_{10} + \tilde{f}_4 F^c_4 + \tilde{f}_6 F^c_6 \\ &+ \tilde{f}_8 F^c_8 + \tilde{f}_{10} F^c_{10} + \tilde{f}_{11} F^c_{11}\} \qquad (5.4)\end{aligned}$$

$$\frac{d\sigma^{\gamma q,Q_2}_{\rm Br}}{dvdw} = Le_q^2\{e_1 + f_{12}F_{12} + f_{13}F_{13} + f_{14}F_{14} + \tilde{f}_{16}F^c_{16} + \tilde{f}_{17}F^c_{17} + \tilde{f}_{20}F^c_{20}\} \qquad (5.5)$$

$$\begin{aligned}\frac{d\sigma^{\gamma q,Q_3}_{\rm Br}}{dvdw} &= Le_Q e_q\{e_1 + \frac{2S_2}{s_2(s+t)}\ln\frac{S_2}{m^2}\ e_4 + e_8 I_{10} + \tilde{f}_4 F^c_4 + \tilde{f}_6 F^c_6 + f_{12}F_{12} \\ &+ f_{14}F_{14} + \tilde{f}_{16}F^c_{16} + f_{18}F_{18} + \tilde{f}_{19}F^c_{19} + \tilde{f}_{20}F^c_{20} + \tilde{f}_{21}F^c_{21}\} \qquad (5.6)\end{aligned}$$

with

$$L = \alpha\alpha_s^2 \frac{1}{N_C}\frac{v}{8\pi}\frac{\tilde{s}_2}{S_2}$$

We do not write down expressions containing $1/\varepsilon$ poles coming from sets Q_1 and Q_2 as they are equal with an opposite sign to the corresponding counterterms with $(S_2 m^2/s_2^2)^\varepsilon$ instead of $(m^2/M_F^2)^\varepsilon$ (see below).

The singularities arise when the final light quark is collinear with the initial one ($k\cdot p_2 = 0$, Fig. 2B, graphs (a), (b)) as well as when the photon is collinear with the light quark ($k\cdot p_1 = 0$, Fig. 2B, graphs (c), (d)). To eliminate them we introduce two counterterms. In the second case the counterterm involves the Born cross section for $\vec{q}\vec{\bar{q}} \to Q\bar{Q}$, which is proportional to [17]:

$$\Delta B_{q\bar{q}}(s,t,u) = -B_{q\bar{q}}(s,t,u) = -\frac{1}{s}\left(\frac{t^2+u^2}{s^2} + 2\frac{m^2}{s}\right) \qquad (5.7)$$

Moreover, in n dimensions, in the t'Hooft-Veltman scheme:

$$\Delta P^n_{gq}(x,\varepsilon) = C_F\{2 - x + 2\varepsilon(1-x)\} \qquad P^n_{gq}(x,\varepsilon) = C_F\{\frac{1+(1-x)^2}{x} - \varepsilon x\}$$

and

$$\Delta P^n_{q\gamma}(x,\varepsilon) = x - \frac{1}{2} - \varepsilon(1-x) \qquad P^n_{q\gamma}(x,\varepsilon) = \frac{x^2+(1-x)^2}{2} - \varepsilon x(1-x)$$

Thus, in the $\overline{MS}$ scheme, the first counterterm gives:

$$[\Delta]\frac{d\sigma^{(1)}_{\rm ct}}{dvdw} = \frac{1}{\varepsilon}\frac{2sv}{1-vw}F(\varepsilon)[\Delta]P_{gq}(x_2)[\Delta]B(x_2 s, t, x_2 u)\left(\frac{m^2}{M_F^2}\right)^\varepsilon, \qquad (5.8)$$

where $F(\varepsilon)$, x_2 and $[\Delta]B$ given by (3.6), (4.8) and (2.5), and the second gives:

$$[\Delta]\frac{d\sigma_{\rm ct}^{(2)}}{dvdw} = \frac{1}{\varepsilon}\frac{16s}{9}F(\varepsilon)\frac{e_q^2}{e_Q^2}[\Delta]P_{q\gamma}(w)[\Delta]B_{q\bar{q}}(ws,wt,u)\left(\frac{m^2}{M_F^2}\right)^{\varepsilon} \tag{5.9}$$

Although not necessary, it is now customary and even advantageous [8] to average the unpolarized cross section over $n-2$ spin degrees of freedom for every incoming boson. This convention is employed when fitting the unpolarized structure functions. As a result, for the unpolarized case, the r.h. side of (5.8) should be multiplied by $(1+\varepsilon)$ and of (5.9) by $(1-\varepsilon)$.

We note that, upon integration, the singular terms in $[\Delta]Q_3$ cancel out, as they should since there is no counterterm proportional to e_qe_Q.

Conversion terms are also needed in the present case. Along the lines of the previous section:

$$[\Delta]\frac{d\sigma_{\rm conv}^{(1)}}{dvdw} = -\frac{2sv}{1-vw}F(0)[\Delta]P_{gq}^{\varepsilon}(x_2)[\Delta]B(x_2s,t,x_2u) \tag{5.10}$$

and

$$[\Delta]\frac{d\sigma_{\rm conv}^{(2)}}{dvdw} = -\frac{16s}{9}F(0)\frac{e_q^2}{e_Q^2}[\Delta]P_{q\gamma}^{\varepsilon}(w)[\Delta]B_{q\bar{q}}(ws,wt,u) \tag{5.11}$$

Finally, we have carried our analytical calculations using REDUCE [18] and to some extent FORM [19].

VI. PHYSICAL CROSS SECTIONS

Here we present the necessary formulas needed for calculation of the differential and total cross sections for the physical process $\gamma p \to Q + X$. This includes derivation of physical cross sections for both components of the reaction, i.e. pointlike and resolved, the latter to leading order (LO). Note we always observe a heavy quark in the final state. Capital letters in this chapter refer to the kinematic variables of the physical process and small letters to those of the subprocess. Starting with the pointlike component, the total cross section for the reaction (1.1) can be written

$$[\Delta]\sigma_{\gamma p}(S) = \int_{x_{min}}^{1} dx\ [\Delta]f_{b/p}(x,Q^2)[\Delta]\hat{\sigma}_{\gamma b}(s); \tag{6.1}$$

b denotes the corresponding parton, $f_{b/p}$ its probability distribution and

$$s = xS, \qquad x_{min} = 4m^2/S. \tag{6.2}$$

The total partonic cross section $[\Delta]\hat{\sigma}_{\gamma b}(s)$ can be calculated straightforwardly by

$$[\Delta]\hat{\sigma}_{\gamma b}(s) = \int_{v_{min}}^{v_{max}} dv \int_{w_{min}}^{1} dw\ [\Delta]\frac{d\hat{\sigma}_{\gamma b}(s,v,w)}{dvdw}, \tag{6.3}$$

where

$$v_{max/min} = \frac{1}{2}(1 \pm \beta), \qquad w_{min} = \frac{m^2}{sv(1-v)}. \tag{6.4}$$

To derive the transverse momentum differential cross section we note that the transverse momentum p_T of a heavy quark is invariant under boosts along the beam axis; also, that our heavy quark rapidities are defined with respect to the *photon*. Consequently we have:

$$[\Delta]\frac{d\sigma_{\gamma p}(S, p_T)}{dp_T} = \int_{x_{min}(p_T)}^{1} dx\ [\Delta]f_{b/p}(x, Q^2)[\Delta]\frac{d\hat{\sigma}_{\gamma b}(s, p_T)}{dp_T}, \tag{6.5}$$

with

$$x_{min}(p_T) = 4(p_T^2 + m^2)/S, \tag{6.6}$$

$$[\Delta]\frac{d\hat{\sigma}_{\gamma b}(s, p_T)}{dp_T} = \int_{y_{min}}^{y_{max}} dy\ \frac{2p_T}{sv}[\Delta]\frac{d\hat{\sigma}_{\gamma b}(s, v, w)}{dvdw}. \tag{6.7}$$

The integration limits on the c.m. rapidity y are

$$y_{max} = -y_{min} = \ln(\sqrt{w_m^{-1}} + \sqrt{w_m^{-1} - 1}),$$

with $w_m \equiv 4(p_T^2 + m^2)/s$. Integration over rapidities in (6.7) is not well defined for "plus" distributions (given in (4.7)) in the partonic cross section. The problem is solved with a change of variables; One needs to consider an integration contour for a heavy quark rapidity y and split it into two parts that no overlapping (i.e. double counting) occurs. Formally one would have

$$\int_{-y_{max}}^{y_{max}} dyf(y) = \int_{-y_0}^{y_{max}} dyf(y \to -y) + \int_{y_0}^{y_{max}} dyf(y). \tag{6.8}$$

In particular, the splitting point y_0 must be the point where function $w = f(y)$ has a minimum. We find

$$y_0 = \ln(2\sqrt{(p_T^2 + m^2)/s})$$

and the general relation between the "new" variable w and the old variable y is

$$\mathrm{e}_{1,2}^{-y} = \frac{1}{2\sqrt{\frac{p_T^2+m^2}{s}}}\left\{1 \pm \sqrt{1 - \frac{4(p_T^2 + m^2)}{sw}}\right\}. \tag{6.9}$$

The correct sign in (6.9) is different in different integration regions, e.g. in the region $[y_0, y_{max}]$ the function e^{-y} decreases when one goes from y_0 to y_{max}, thus minus sign in (6.9). Similarly, we find that for the first term of (6.8) the sign for e^{-y} in (6.9) should be positive. The resulting expression for the p_T differential cross section reads:

$$[\Delta]\frac{d\hat{\sigma}_{\gamma b}(s, p_T)}{dp_T} = \int_{w_m}^{1} \frac{dw}{w}\frac{2p_T}{s\sqrt{1 - w_m/w}}\left\{[\Delta]\frac{d\hat{\sigma}}{dvdw}(v = v_+) + [\Delta]\frac{d\hat{\sigma}}{dvdw}(v = v_-)\right\}, \tag{6.10}$$

where

$$v_\pm = \frac{1}{2}(1 \pm \sqrt{1 - w_m/x}). \tag{6.11}$$

However, even the expression (6.10) is not well suited for numerical integration. One notices that there is a numerically divergent (though analytically integrable) square root in the denominator. The singularity comes from the lower limit $x_{min}(p_T)$ of the x integration. To avoid this minor problem one more change of variables is necessary. Instead of the old variables x, w we introduce the new variables z, w' through the relations

$$z = \sqrt{1 - \frac{x_{min}(p_T)}{wx}}, \qquad w' = w. \tag{6.12}$$

To correctly define integration limits for the new variables one has to perform a nontrivial mapping. Finally we obtain:

$$[\Delta]\frac{d\sigma_{\gamma b}(S, p_T)}{dp_T} = \frac{4p_T}{Sx_{min}(p_T)} \int_0^{z_m} dz \int_{w'_m}^1 dw\, [\Delta]F_{b/p}(x, Q^2) \left\{ [\Delta]\frac{d\hat{\sigma}}{dvdw}(v_+) + [\Delta]\frac{d\hat{\sigma}}{dvdw}(v_-) \right\}. \tag{6.13}$$

$F_{b/p}(x, Q^2)$ is a momentum distribution and

$$z_m = \sqrt{1 - x_{min}(p_T)}, \quad w'_m = \frac{x_{min}(p_T)}{1 - z^2}, \quad x = \frac{w'_m}{w}. \tag{6.14}$$

For the rapidity Y fixed one gets the following expression:

$$[\Delta]\frac{d\sigma_{\gamma p}(S, Y)}{dY} = \int_{x_{min}(Y)}^1 dx\ [\Delta]f_{b/p}(x, Q^2)[\Delta]\frac{d\hat{\sigma}_{\gamma b}(s, y)}{dy}, \tag{6.15}$$

with

$$x_{min}(Y) = \mathrm{e}^{-Y}/(\sqrt{S}/m - \mathrm{e}^Y), \tag{6.16}$$

and

$$[\Delta]\frac{d\hat{\sigma}_{\gamma b}(s, y)}{dy} = \int_{w_{min}}^1 \frac{2wdw}{(\mathrm{e}^y + w\mathrm{e}^{-y})^2}[\Delta]\frac{d\hat{\sigma}}{dvdw} \tag{6.17}$$

$$w_{min} = \frac{\mathrm{e}^y}{\sqrt{s}/m - \mathrm{e}^{-y}}, \quad v = \frac{1}{1 + w\mathrm{e}^{-2y}}, \quad y = Y + \frac{1}{2}\ln x.$$

Finally we turn to the resolved LO photon contributions. We define the doubly differential cross section $d\sigma/dYdp_T$ for the $2 \to 2$ subprocess:

$$[\Delta]\frac{d\sigma_{\gamma p}}{dYdp_T} = 2p_T \int_{x_{1,min}}^1 dx_1 \frac{[\Delta]F_{a/\gamma}(x_1, Q^2)[\Delta]F_{b/p}(x_2^0, Q^2)}{x_1 - \mathrm{e}^Y A}[\Delta]\hat{\sigma}_{ab}(s, x_1, x_2^0), \tag{6.18}$$

where

$$x_2^0 \equiv \frac{x_1\mathrm{e}^{-Y}A}{x_1 - \mathrm{e}^Y A}, \quad A \equiv (\frac{p_T^2 + m^2}{S})^{1/2}, \quad s = x_1x_2^0S. \tag{6.19}$$

The expressions (6.1) - (6.19) give all the formulas we have used.

VII. NUMERICAL RESULTS

We present results for Q=c-quark ($m_c = 1.5$ GeV) at $\sqrt{S_{\gamma p}} \equiv \sqrt{S} = 10$ GeV, relevant to the experiments [1] and $[2,(a)]$ and $\sqrt{S} = 100$ GeV, as well as for Q=b-quark ($m_b = 5$ GeV) at $\sqrt{S} = 100$ GeV; the later energy is relevant to HERA. Higher HERA energies are not considered as the cross sections become too small. The effect of changing m_c is also considered.

We use the NLO sets of polarized parton distributions of [20], which can be characterized in terms of the polarized gluon distribution $\Delta g\,(x)$ as follows:

Set A: $\Delta g\,(x) > 0$ and relatively large

Set B: $\Delta g\,(x) > 0$ and small

Set C: $\Delta g\,(x)$ changing sign; $\Delta g\,(x) < 0$ for $x > 0.1$.

Notice that in the presented results also the LO contribution is convoluted with NLO distributions; in this way we believe that e.g. the magnitude of K-factors more properly reflects the NLO subprocess terms. Also, we use throughout the NLO expression of $\alpha_s\,(\mu)$ with the values for the QCD scale Λ, flavor thresholds and number of active flavors $N_{lf} = N - 1$ that match the definitions corresponding to heavy quark decoupling. We note that in [5] the above values were taken to match the definitions for the respective parton distributions. However, we have explicitly verified that this amounts to a negligible change in the final numerical results. Note, in (2.8) we take $M = m$.

At this moment there is no experimental information on the polarized photon structure functions $\Delta F_{q/\gamma}$ and $\Delta F_{g/\gamma}$, which determine the resolved γ contributions. To estimate them we have used the LO maximal and minimal saturation sets of [21], as well as the sets of [22], which belong to the class of the so-called asymptotic solutions. The two sets of [21] give contributions differing little, with the maximal saturation one slightly exceeding; the results presented below correspond to this set. The largest resolved contributions come from [22].

In Figs. 3I, II and III, at $\sqrt{S} = 10$ and 100 GeV we present quantities related with the differential cross sections $\Delta d\sigma/dp_T$, where $p_T = p_{3T}$ (Fig. 1), versus $x_T \equiv 2p_T/\sqrt{S}$. Measurement of such cross sections at $\sqrt{S} \approx 10$ GeV may be carried in (a) of [2]. Here we use the renormalization and factorization scale $\mu = M_f = \left(p_T^2 + m^2\right)^{1/2}$.

In the parts (a) of Figs. 3I, II and III we present the NLO and LO (denoted by a $*$) contributions to the physical differential cross section for sets A, B and C of [20]. For set B we also present the contribution of subprocess (1.3) and of the resolved photon.

In the parts (b) of the same Figs we present the asymmetries

$$A_{LL}(p_T) = \frac{\Delta d\sigma/dp_T}{d\sigma/dp_T} \tag{7.1}$$

The unpolarized distributions are the most recent set, CTEQ5 [23]. In A_{LL} the resolved γ contributions have been left out since they are small and what is presently known does not permit a completely scheme independent calculation. The errors have been estimated using

$$\delta A_{LL} = \frac{1}{P_B P_T \sqrt{L\sigma\epsilon}} \tag{7.2}$$

At $\sqrt{S} = 10$ GeV we use the conditions of [1] ($P_B = 80\%$, $P_T = 25\%$, $L = 2\ fb^{-1}$, c-quark detection efficiency $\epsilon_c = 0.014$) and unpolarized cross section σ integrated over a bin of x_T corresponding to $\Delta p_T = 0.5$ GeV. At $\sqrt{S} = 100$ GeV we use $P_B = P_T = 70\%$, $L = 100$ pb^{-1}, $\epsilon_c = 0.15$, for b-quark $\epsilon_b = 0.05$ and σ integrated over a bin corresponding to $\Delta p_T = 5$ GeV.

Figs. 3I(a) and 3II(a) show that between $\sqrt{S} = 10$ and 100 GeV the shape of the LO $\Delta d\sigma_{LO}/dp_T$ and NLO $\Delta d\sigma/dp_T$ varies dramatically; this also holds for the K-factor, $K = \Delta d\sigma/dp_T/\Delta d\sigma_{LO}/dp_T$.

Most impotrant is the possibility to distinguish between sets A, B and C. Fig. 3I(b) shows that at $\sqrt{S} = 10$ GeV near $x_T = 0.3$ one can distinguish A and C and perhaps all A, B, C. Figs. 3II(b) and 3III(b) show that at $\sqrt{S} = 100$ GeV the best range is $0.2 \leq x_T \leq 0.3$; and for $Q = c$ one may distinguish all A, B, C, but for $Q = b$ only A and C.

In Figs. 4I, II and III we present rapidity distributions. Here we use $\mu = M_f = 2m$. The presented differential cross sections are analogous to those of Figs. 3I, II and III and

$$A_{LL}(Y) = \frac{\Delta d\sigma/dY}{d\sigma/dY} \tag{7.3}$$

The errors have been estimated using (7.2) where now the unpolarized cross sections σ are integrated over a bin $\Delta Y = 1$.

Fig. 4I(b) shows that at $\sqrt{S} = 10$ GeV the region $1.25 \leq Y \leq 1.5$ is the best to distinguish set C from A or B. Fig. 4II(b) shows that at $\sqrt{S} = 100$ GeV for c-quark, $A_{LL}(Y)$ has become too small. At $Y \approx -1$ it seems one can distinguish all A, B, C, but $\Delta d\sigma/dY$ is small for all sets (Fig. 4II(a)). Perhaps more promising is the range $0 \leq Y \leq 1$, where one can distinguish C from A or B. Finally Fig. 4III(b) shows that detection of b-quark is not useful due to large errors (ϵ_b small).

Figs. 5I,II and III present integrated cross sections $\Delta\sigma$ and the corresponding asymmetries $A_{LL} = \Delta\sigma/\sigma$ versus the c.m. energy $\sqrt{S}$. The scale is again $\mu = M = 2m$.

Comparison of Figs. 5I and 5II shows that at the two different ranges of $\sqrt{S}$ the changes in the shapes and signs of $\Delta\sigma$ and A_{LL} is again dramatic; clearly the same holds for the corresponding K-factors, $K = \Delta\sigma_{NLO}/\Delta\sigma_{LO}$.

In Fig. 5I(b) the error (at $\sqrt{S}$=10 GeV) is estimated using again in (7.2) the conditions of [1]. Under these conditions we conclude that sets A and C can be distinguished, but not sets A and B or B and C. The proposed SLAC experiment [2a], which amounts to better conditions, and will give results at somewhat lower $\sqrt{S}$, may distinguish also B and C.

In Figs. 5II(b) and 5III(b) the errors (at $\sqrt{S}$=100 GeV) have been estimated using again the values of $P_B, P_T, L, \varepsilon_c$ and ε_b stated after Eq. (7.2). For c-quark, $\mid A_{LL} \mid$ are very small due to relatively large unpolarized cross sections σ. For the same reason, however, the error δA_{LL} is not very large, so set C can be distinguished from A or B. For b-quark, due to a combination of small ε_b and rather small σ, the error is very large and precludes any useful information on Δg.

Finally, Fig. 6, for the integrated NLO cross sections $\Delta\sigma$ and σ and for the asymmetries $A_{LL} = \Delta\sigma/\sigma$, shows the effect of changing the c-quark mass m_c (part (a)) and the scales μ, M_f (part (b)). The results refer to set B of [20]. E.g. regarding $\Delta\sigma$, in Fig. 6(a) we define

$$R_m = \frac{\Delta\sigma(m_c) - \Delta\sigma(1.5 \text{ GeV})}{\Delta\sigma(1.5 \text{ GeV})}, \tag{7.4}$$

and in Fig. 6(b), keeping $\mu = M_f$, we define

$$R_{SC} = \frac{\Delta\sigma(\mu) - \Delta\sigma(2m_c)}{\Delta\sigma(2m_c)}; \tag{7.5}$$

similarly for σ and A_{LL}. Fig. 6(a) shows that at the lower $\sqrt{S}$ the effect of changing m_c is more pronounced.

VIII. COMPARISON WITH OTHER PUBLICATIONS

Figs. 3II(b) and 3III(b) show that at small x_T, $A_{LL}(p_T)$ is small; the same holds for $A_{LL}(Y)$ of Fig. 4II(b). This may lead one to conclude that HERA is rather useless in specifying Δg [5]. However, it may not be so. On the basis of Figs. 3II(b) and III(b), reconstruct events and select only those with, say, $x_T > 0.2$, i.e. carry integrations of $\Delta d\sigma/dp_T$ over some cut phase space. This may well enhance the resulting A_{LL} [24].. Of course, an estimate of the corresponding errors is required to reach a definite conclusion.

Finally, since we present analytic results for the unpolarized cross section as well, we will compare with similar results of [8] ("soft" part, Eq. (2.24) of [8]); here the relevant part is the last three lines of Eq. (4.5). Ref. [8] uses the phase space slicing method, which separates the soft and hard gluon parts via a cut parameter Δ. The formal relation with our approach is

$$\frac{sv}{m^2} \to \Delta; \tag{8.1}$$

the necessary framework to relate these two methods is developed in [25]. Now, concerning terms involving t and u, we easily see that they are exactly the same, except that t and u are interchanged (c.f. our definition, Eq. (2.1) with that of [8], Eq. (2.13)). The only difference seems to arise from the coefficient of $\zeta(2)$, which is -2 in our case versus $-3/2$ in [8]. Note, however, that our coefficient $F(\varepsilon)$ in (3.6) contains $\Gamma(1+\varepsilon)$, which upon expansion in powers of ε, gives a term $(\varepsilon^2/2)\,\zeta(2)$; this accounts for the difference. Since $F(\varepsilon)$ appears both in our loop contribution (3.6) and in our Brems contribution (4.7), the overall result is unaffected. To verify our calculation we have evaluated numerically the NLO $\overline{MS}$ scaling functions for the partonic γg cross section, taking into account an additional "mass" factorization term given in eq. (6.31) of [12], and compared it to the corresponding curves of Fig. 5 of [8]. We found exact agreement. We have also explicitly verified that the sum of our non-Abelian loop contributions and the Brems ones, that are proportional to the Born contribution, equal analytically the corresponding "virtual+soft" expression presented in [5].

IX. CONCLUSIONS

In this paper we have presented the complete analytic results for the heavy flavor photoproduction for both, longitudinally polarized and unpolarized initial particles, in a closed form. These include the NLO contributions of the hard Brems due to the relevant partonic subprocesses (1.2) and (1.3) that are presented for the first time in analytic form. We have computed numerically various total and differential cross sections for the energy ranges of CERN, SLAC and HERA. We have discussed the possibilities to differentiate between various scenarios for the polarized gluon distribution Δg and have once more emphasized the way to enhance the asymmetries for HERA energies by measuring the differential cross sections with the help of certain acceptance cuts (see also our earlier Ref. (*a*) of [24] on this subject).

ACKNOWLEDGEMENTS

We thank I. Bojak for his kind collaboration in doing comparisons. Thanks are also due to G. Bunce, D. de Florian, B. Kamal and J. Körner for discussions, to W. Vogelsang for discussions and for providing us the sets of [19], to P. Bosted for several communications, to A. Despande for useful information and remarks and to V. Spanos and G. Veropoulos for participating in part of the calculations. Z.M. would like to thank the Particle Theory group of the Institut für Physik, Universität Mainz, for hospitality, where the calculations of the final parts of this paper were carried out.

APPENDIX A

Here we present the coefficients of the loop contributions. In the following $[\Delta]A_i$, i=1,3, are given in App. B of [6]. For $[\Delta]d\sigma_{a-e}/dv$ given in Eq. (3.2):

$$\begin{aligned}
\Delta\tilde{A}_1 &= \Delta A_1; \quad \Delta\tilde{A}_2 = -4[2(7s^2/t^2+8s/t+6)m^2/u+11s^2/tu+24s/u+26t/u+ \\
&\qquad 12t^2/su+st/uT-2t^2/sT]m^2/T \\
\Delta\tilde{A}_3 &= \Delta A_3/2; \quad \Delta\tilde{A}_4 = 4[(2u/t-s/u)m^2/t-2s/t+2u/s]m^2/T
\end{aligned}$$

$$\begin{aligned}
\tilde{A}_1 &= A_1; \quad \tilde{A}_2 = 4[(24s/t - 2s^2/tT + 2s/T + 12t/T)m^4/tu + (s/t + 6t/s + t/T + 11) \\
&\qquad\qquad m^2s/uT - 2t^2/T^2] \\
\tilde{A}_3 &= A_3/2; \quad \tilde{A}_4 = -4[4m^4s/ut^2 - (2s^2/t^2 - s/t + t/T - 2)m^2/u - t/T] \qquad \text{(A1)}
\end{aligned}$$

For $[\Delta]d\tilde{\sigma}_g/dv$ and $[\Delta]d\sigma_g/dv$ given in Eqs. (3.5) and (3.7):

$$\begin{aligned}
\Delta A'_1 &= m^2s/t^2 \\
\Delta A'_2 &= 4[2m^4s^2/Tut^2 - (8su/t^2 + 9u/T - 8 - t/T - 8t^2/sT - st/T^2 + 2t^2u/sT^2)m^2/u] \\
\Delta A'_3 &= 4[m^4s/Tut - 2(s/t - 1 - t^2/sT)m^2/t] \\
A'_1 &= -m^2s^2/t^2u - 1 \\
A'_2 &= -4[(16sT/t^2 + 2s^2/t^2 + 8 - u/T + t/T)m^4/uT + 2(s/u - 2s/T)m^2/t] \\
A'_3 &= 4[(4sT/t^2 + s/t + 2)m^4/uT + 2m^2s^2/ut^2 + 3] \qquad \text{(A2)}
\end{aligned}$$

For $[\Delta]d\tilde{\sigma}_h/dv$ and $[\Delta]d\sigma_h/dv$ given in Eqs. (3.9) and (3.10):

$$\begin{aligned}
\Delta B'_1 &= 2[4(5/u + 1/t)m^4/t + (5/u + 7/t + 4u/t^2)m^2 + (4/u + 3/t)(t^2 + u^2)/s] \\
\Delta B'_2 &= -(15s^2/tu - 62)m^2s/tu - 4(s^2/tu + 8)m^4/tu + 13/4(s^2/tu - 2) \\
\Delta B'_3 &= 2[(3/u + 4/t)(u - t)m^2/t + (1/s - 1/t)(t^2 + u^2)/u] \\
\Delta B'_4 &= 4[2(2/u + 3/t + u/t^2)m^2 - (t^2/u - t + 9u + 3u^2/t - 6tu/T - t^4/T^2u + t^3/T^2)/s] \\
\Delta B'_5 &= 8(s^2/tu - 3)m^2s/tu \\
\Delta B'_6 &= 2[2(1/T + 1/U)m^2/s + 2(t^2/u^2 + u^2/t^2 + 2t/u + 2u/t)/s - t/uU - u/tT - \\
&\quad (t^3/u - 2tu + u^3/t)/sTU]m^2 \\
B'_1 &= 2[4(1/t - 3/u)m^4/t - (1 - u/t)(1/u + 2/t)m^2 + 4t/u + 2 + 3u/t] \\
B'_2 &= [4(29/u^2 - 6/tu + 29/t^2)m^4 - 2(1/u^2 - 12/tu + 1/t^2)m^2s - 13t/u + 4 - 13u/t]/4 \\
B'_3 &= 2[4(1/t - 3/u)m^4/t + (2u/t^2 - 1/t - 5/u)m^2 - 2s/u + u/t] \\
B'_4 &= -4[2(4/u + 1/t)m^2s/t + 4t/u - 3s/t - 2t^2/Tu - t/T - 2t^3/T^2u] \qquad \text{(A3)} \\
B'_5 &= -16(1/t^2 + 1/u^2)m^4 \\
B'_6 &= -4[(t/Uu^2 + u/Tt^2)m^4 - (5s/tu - 1/U - 1/T - t^2/TUu - u^2/TUt)m^2 + 2tu/TU]
\end{aligned}$$

APPENDIX B

In this Appendix we list the coefficients of the Brems contributions. For $\Delta G^{\gamma g}$ given in Eq. (4.3) and $\Delta d\sigma_{\rm Br}^{\gamma g}/dvdw$ given in Eq. (4.5), the coefficients Δe_i and Δf_i are

$$\begin{aligned}
\Delta e_1 &= 16[4(s/s_2u - 1/u + 1/t)m^2/t + 3s/s_2u - 2/u - s/s_2t - s_2/tu - u/s_2t] \\
\Delta e_2 &= 8[8(-s/u - 1 + s/t)m^4/s_2t + 2(2s/u - 2 + 4s/t - 3ss_2/t(s+u))m^2/s_2 - \\
&\quad 4s^2/s_2u + 4s/u - 2s/s_2 - u/s_2 + u/t + 2ss_2/tu + 3u/(s+u)]
\end{aligned}$$

$$
\begin{aligned}
\Delta e_3 &= 0; \qquad \Delta e_4 = 8[4(s/u + s/s_2 - t/s_2)m^2/t + ss_2/tu + su/s_2t - 2u/s_2 - 2] \\
\Delta \tilde{e}_5 &= 8[8(t/u + 1)m^4/s_2t - 2(s^2/s_2u + s/u + 4t/s_2 - 2s_2/u)m^2/t + st/s_2u + \\
&\quad 4s/s_2 - 2 + su/s_2t + 2u/t] \\
\Delta \tilde{e}_6 &= 4[8(s/u - s_2/t + u/t)m^4/s_2 + 2(2st/s_2u + s/s_2 - s_2/u + 2 + 2ss_2/tu - \\
&\quad 2s^2/s_2t)m^2 + s(s^2 + u^2)/s_2t] \\
\Delta e_7 &= 4[8(s_2/u - 1)m^4/t + 2(2s/u + 3 - s_2/s - 2s_2^2/tu + 2s/t)m^2s/(s + u) - \\
&\quad ss_2(s^2 + s_2^2)/t(s + u)u]; \qquad \Delta e_8 = 16(s_2/u - u/s_2)/t \\
\Delta \tilde{e}_9 &= 4[8(t/u + s/t)m^4/s_2 - 2(2s^2/s_2u - 2s/u + 2s_2/u - 2 + (st/s_2 + 2su/s_2 - \\
&\quad s_2)/(s + u))m^2 - st(2s/s_2u - 2/u + (s_2/u + u/s_2)/(s + u))] \\
\Delta e_{10} &= 16(t/u - u/t)/s_2; \qquad \Delta e_{11} = -16m^4s/u \\
\Delta f_1 &= 16[4(s/u - 1)m^2/s_2t + (3/s_2 + 1/t)s/u]; \qquad \Delta f_2 = 32(s + u)/ts_2u \\
\Delta \tilde{f}_3 &= \Delta f_2; \qquad \Delta \tilde{f}_4 = -32[(2/s_2 + 2/t - s/s_2u)m^2/t + 1/t + 1/s_2] \\
\Delta \tilde{f}_5 &= 8[2(s/s_2u + s/tu - 2u/t^2 + s/t(s + u) - 4ss_2/t^2(s + u))m^2 - s^2/s_2u + \\
&\quad 2s/u - 2s/s_2 + 2 - 2u/s_2 + ss_2/tu + s_2/t + (u + 2s_2u/t)/(s + u)] \\
\Delta \tilde{f}_6 &= 4[2(2s^2/s_2u + s/u + s_2/u + 3s/s_2 + (s + 2su/s_2 - 3s_2 - 4s(s_2^2 + \\
&\quad u^2)/tu)/(s + u))m^2 + s^2/s_2 + 2su/s_2 + 2u^2/s_2 - 2s^2/t - 4su/t + \\
&\quad 2s_2^2/t - 2u^2/t + (s_2^2 + u^2)/(s + u)] \\
\Delta \tilde{f}_7 &= 0; \qquad \Delta \tilde{f}_8 = 0 \\
\Delta \tilde{f}_9 &= 4[2(2s/u - 2s_2^2/tu + s_2/t - (ss_2/u + 2su/t - s_2u/t)/(s + u))m^2 + s_2 - \\
&\quad 2t - s_2^2/t - u^2/t + (s_2^2 + u^2)/(s + u)] \\
\Delta \tilde{f}_{10} &= -8(2s + t)m^2; \qquad \Delta \tilde{f}_{11} = 0 \qquad\qquad \text{(B1)}
\end{aligned}
$$

For $G^{\gamma g}$ given in Eq. (4.3) and $d\sigma^{\gamma g}_{\rm Br}/dvdw$ given in Eq. (4.5), the coefficients e_i and f_i are

$$
\begin{aligned}
e_1 &= 16[4(1/s_2u + 1/s_2t - 1/t^2)m^2 - 3s/s_2u + 2/u - 1/s_2 - s_2/tu - 1/t] \\
e_2 &= 8[-16(1/t + 1/u)m^6/s_2t - 8(3t/s_2u + 2/u + 2/s_2 - 1/(s + u))m^4/t + \\
&\quad 2(s^2/s_2u - 8s/u + 4s/s_2 - 1 + 2u/s_2 - 3s_2/t + u/t)m^2/(s + u) + u/s_2 - \\
&\quad 4st/s_2u - 2s/s_2 + (2s_2 - 2u + 2ss_2^2/tu + s_2u/t)/(s + u)] \\
e_3 &= -16m^2 \\
e_4 &= -8[8m^4(1/u + 1/s_2) - 2m^2(s/u - s/s_2 - 2s_2/u - 2u/s_2) + (s_2 + u)(2 + \\
&\quad 2u/s_2 + 2s/s_2 - s/u + s/s_2)]/t \\
\tilde{e}_5 &= 8[8(s/s_2 - 1)m^4/tu - 2m^2(s/s_2u + 2/u - 5/s_2 + 3/t - u/ts_2) + s^2/s_2u - s/u - \\
&\quad s/s_2 + 4 + su/ts_2 - 2s_2/t + 2s^2/ts_2] \\
\tilde{e}_6 &= 4[16m^6(1/su - 1/s_2u - 1/ts_2) + 8(su - (s - s_2)^2 - (s_2 - u)^2)m^4/ts_2u + 2m^2(t/u + \\
&\quad s/s_2 - 1 + s/t) - s(s^2 + u^2)/s_2t] \\
e_7 &= 4[16(s_2/u - 1)m^6/st + 8(s^2 + ss_2 + s_2^2)m^4/tu(s + u1) + 2m^2(3s/t + (ss_2/u - s_2 -
\end{aligned}
$$

$$
\begin{aligned}
& 2ss_2/t)/(s+u)) - ss_2(s^2+s_2^2)/tu(s+u1)]; \qquad e_8 = 16(s_2+u)^2/ts_2u \\
\tilde{e}_9 &= 4[16(s/s_2 - 2 + s_2/s - u/s)m^6/tu + 8(s_2/u - 3st/s_2u - 2 + u/s_2)m^4/(s+u) + 2m^2 \times \\
& ((s-s_2)(1/u + 1/s_2) - 1 + 2(s_2 - s)/(s+u)) + (s_2/u - 2 + u/s_2 - 2st/s_2u)st/(s+u)] \\
e_{10} &= -16(1/t - 1/u)(s/s_2 - 1); \qquad e_{11} = 32m^6/u \\
f_1 &= -16[8m^4/ts_2u + 2(2/u + s/tu)m^2/s_2 + s/u(1/t + 3/s_2) - 2ss_2/t(s+u)u] \\
f_2 &= 32(1/t + 1/s_2)/u; \qquad \tilde{f}_3 = f_2 \\
\tilde{f}_4 &= -32[4m^4/ts_2u + 2(1/s_2 + 1/t)m^2/u - 1/s_2 + s_2/t(s+u)] \\
\tilde{f}_5 &= -8[8m^4(1/s_2u + 1/tu + (1/t - 2s_2/t^2)/(s+u)) - 4m^2(1/t + 2s_2/t^2 - (st/s_2 + \\
& ss_2/t)/(s+u)u) - t/u + 2t/s_2 - s_2^2/tu + (s^2t/s_2u + 2u - 2s_2u/t)/(s+u)] \\
\tilde{f}_6 &= 4[8m^4(s^2/ts_2u - 1/s_2 - 4/t - (s/t - s_2s/ut - s_2u)/(s+u)) + 4(s^2/s_2 + su/s_2 - \\
& 2s_2 + s - u - s_2(s+s_2)/(s+u))m^2/t - (1 - (s_2^2 + u^2)/(s+u1)t)(s + s_2 + u)^2/s_2] \\
\tilde{f}_7 &= -32(s+u)^2m^2/t^2; \qquad \tilde{f}_8 = 32(s+u)m^2u/t \\
\tilde{f}_9 &= 4[8m^4(s^2/tu + s_2/u + s_2/t) + 4m^2(ss_2/t + s_2 - 2s) + (s_2/t - 2)(s_2^2 + u^2 - st - \\
& ut)]/(s+u); \qquad \tilde{f}_{10} = 16m^2(2m^2+u); \qquad \tilde{f}_{11} = -8m^2u^2 \qquad \text{(B2)}
\end{aligned}
$$

Now we shall write down the coefficients $[\Delta]e_i$ and $[\Delta]f_j$ for the subprocess $\gamma q \to Q\bar{Q}q$. For Q_1 we have:

$$
\begin{aligned}
\Delta e_1 &= -8(2m^2 - t)/t^2, \quad \Delta e_3 = 0, \quad \Delta e_4 = -8 * s/t, \quad \Delta e_8 = 0 \\
\Delta\tilde{f}_4 &= 8(2m^2 + t)/t^2, \quad \Delta\tilde{f}_5 = 4(2(s_2 + s)m^2 - ut)/t^2 \\
\Delta\tilde{f}_6 &= -2(2m^2 + 2s_2 - t), \quad \Delta\tilde{f}_7 = 0, \quad \Delta\tilde{f}_8 = 0, \quad \Delta\tilde{f}_{10} = 2(2s+t)m^2, \quad \Delta\tilde{f}_{11} = 0 \\
e_1 &= 8(2m^2 + t)/t^2, \quad e_3 = 4m^2, \quad e_4 = 8(2u + s)/t, \quad e_8 = -16/t \\
\tilde{f}_4 &= 8/t, \quad \tilde{f}_5 = -4(4m^4 + 4m^2s_2 + ut)/t^2 \\
\tilde{f}_6 &= 2(4(s_2+u)m^2 + 2(2s + 3t)s_2 + 8m^4 - 4s_2^2 - 2s^2 - 4st - 3t^2)/t \\
\tilde{f}_7 &= 8(s_2 - t)^2m^2/t^2, \quad \tilde{f}_8 = -8u(s_2 - t)m^2/t \\
\tilde{f}_{10} &= -4(m^2 + u)m^2, \quad \tilde{f}_{11} = 2u^2m^2 \qquad \text{(B3)}
\end{aligned}
$$

For Q_2:

$$
\begin{aligned}
\Delta e_1 &= -16/s, \quad \Delta f_{12} = -8/s, \quad \Delta f_{13} = -8m^2/s, \quad \Delta f_{14} = -8(2m^2 + u)/s \\
\Delta\tilde{f}_{15} &= 8t/s, \quad \Delta\tilde{f}_{16} = 2(2u(s+t) - 4m^2s + s^2 + 2ts_2)/s \\
\Delta\tilde{f}_{17} &= 2m^2s, \quad \Delta\tilde{f}_{20} = 0 \\
e_1 &= 16/s, \quad f_{12} = 8/s, \quad f_{13} = 8m^2/s, \quad f_{14} = 8(2m^2 + u)/s \\
\tilde{f}_{15} &= 8(2m^2 + u)/s, \quad \tilde{f}_{16} = -2(4m^2s - 4s_2^2 + 6s_2s + 4s_2t - 3s^2 - 4st - 2t^2)/s \\
\tilde{f}_{17} &= 2m^2s, \quad \tilde{f}_{20} = -16/s \qquad \text{(B4)}
\end{aligned}
$$

And, finally, for Q_3:

$$
\Delta e_1 = 8(s_2 - 2s + t)/st, \quad \Delta e_4 = -8, \quad \Delta e_8 = 0
$$

$$\begin{aligned}
\Delta\tilde{f}_4 &= -8(s_2-t)/st, \quad \Delta\tilde{f}_5 = 4(2(s_2-t)m^2+s_2^2-s_2t-ut)/st \\
\Delta\tilde{f}_6 &= -2(2(2s+t)m^2-2s_2t+t^2)u/(s+t)s, \quad \Delta f_{12} = 8(s_2-s)/st \\
\Delta f_{14} &= 4(2(s_2-3s)m^2-2su+2s_2u+ts_2)/st, \quad \Delta\tilde{f}_{15} = 8 \\
\Delta\tilde{f}_{16} &= -2(2(s+2t)s_2-2m^2s-s^2-4st-2t^2)u/(s+t)t \\
\Delta f_{18} &= -2(2((2s+t)s_2+2s^2+2st)m^2-(2u+t)s_2t)/(s+t)s \\
\Delta\tilde{f}_{19} &= -2(2(s+t)s_2-2m^2s-s^2+2ut)s_2/(s+t)t, \quad \Delta\tilde{f}_{20} = 0, \quad \Delta\tilde{f}_{21} = 0 \\
e_1 &= -8(s_2-2s-t)/st, \quad e_4 = 8(2m^2+s_2+u+tu/(s+t))/s, \quad e_8 = -16/s \\
\tilde{f}_4 &= -8(s_2-t)/st, \quad \tilde{f}_5 = 4(2(s_2-t)m^2+s_2^2-s_2t-ut)/st \\
\tilde{f}_6 &= -2(2(4s/t+t/(s+t))m^2+2s_2+2u+(2s_2t-4s_2^2-t^2)/(s+t))u/s \\
f_{12} &= -8(s_2-s)/st, \quad f_{14} = -4(2(s_2-3s)m^2+2s_2u+s_2t-2su)/st \\
\tilde{f}_{15} &= 8(2m^2+u+ss_2/(s+t))/t \\
\tilde{f}_{16} &= 2(2m^2s-4s_2^2+6s_2s+4s_2t-3s^2-4st-2t^2)u/(s+t)t \\
f_{18} &= -2(2(4su/t+2s-s_2t/(s+t))m^2+s_2(s_2+u-((s-2s_2)^2+2s_2s)/(s+t)))/s \\
\tilde{f}_{19} &= 2(2(s+2t)s_2-2m^2s-4s_2^2-s^2-2st-2t^2)s_2/(s+t)t \\
\tilde{f}_{20} &= -16/t, \quad \tilde{f}_{21} = -16m^2s/t
\end{aligned} \tag{B5}$$

APPENDIX C

We give here the Brems integrals, F_i, $i=1,...,11$, appearing in Eq. (4.5) and also in Eqs. (5.4) - (5.6). Define,

$$P_1 = us_2 - s(t+2m^2), \qquad P_2 = s((t+m^2)(us_2-m^2s)-m^2(s+u)^2) \tag{C1}$$

We may now write down the integrals:

$$\begin{aligned}
F_1 &= -\frac{1}{(s+u)^2}[P_1 + \frac{sS_2}{s_2}(t+2m^2)\ln\frac{S_2}{m^2}] \\
F_2 &= \frac{1}{(s+u)^3}[P_1(\frac{s_2(s+u)(t+u+2m^2)}{4S_2}+s(t+2m^2))+P_2\frac{s_2+2m^2}{2S_2}+\frac{S_2}{s_2} \\
&\times\ (\frac{s^2(t+2m^2)^2}{2}-P_2\frac{m^2}{S_2})\ln\frac{S_2}{m^2}] \\
F_3^s &= -\frac{s_2S_2u^2}{2(s+u)^3} \\
F_3^c &= \frac{s_2}{2S_2(s+u)}[\frac{(t+u)^2}{4}-m^2s-\frac{t+u+2m^2}{s+u}P_1-\frac{3}{4}\frac{P_1^2}{(s+u)^2}] \\
F_4^s &= \frac{S_2u}{(s+u)^2}, \qquad F_4^c = \frac{P_1}{(s+u)^2}, \qquad F_5^s = -\frac{2S_2}{s_2(s+u)}, \qquad F_5^c = 0
\end{aligned}$$

$$\begin{aligned}
F_6^s &= -\frac{4S_2}{s_2ut}, \qquad\qquad F_6^c = \frac{4S_2}{s_2ut}[\ln\frac{S_2}{m^2} + 2\ln\frac{ut}{ss_2+ut}] \\
F_7^c &= -\frac{8S_2^2}{s_2^2(s+u)^2}(1-\varepsilon) \\
F_8^s &= -\frac{16S_2^2}{s_2^2ut(s+u)}\frac{s_2}{2S_2}\frac{s+t}{u^2t^2}(s+u)(ut-2m^2s) \\
F_8^c &= \frac{16S_2^2}{s_2^2ut(s+u)}[\frac{s_2}{2S_2}\frac{s+t}{u^2t^2}(s+u)(ut-2m^2s)(\ln\frac{S_2}{m^2} + 2\ln\frac{ut}{ss_2+ut}) - \frac{s_2^2}{S_2^2}\frac{2P_2}{u^2t^2} - 1 + \varepsilon] \\
F_9^s &= \frac{4S_2}{s_2^2u}, \qquad\qquad F_9^c = -\frac{4S_2}{s_2^2u}[\ln\frac{S_2}{m^2} + \ln\frac{u^2}{(s+u)^2}] \\
F_{10}^s &= -\frac{8S_2(s+u)}{s_2u^2t^2}, \qquad\qquad F_{10}^c = \frac{8S_2(s+u)}{s_2u^2t^2}[\ln\frac{S_2}{m^2} + 2\ln\frac{ut}{ss_2+ut} + \frac{s_2}{m^2}\frac{ut-2m^2s}{ss_2+ut}] \\
F_{11}^s &= -\frac{32S_2^2}{s_2^2u^2t^2}\frac{s_2^2}{S_2^2u^2t^2}[P_2 + \frac{S_2}{s_2}(ss_2+ut)(ut-2m^2s)] \\
F_{11}^c &= \frac{32S_2^2}{s_2^2u^2t^2}[\frac{s_2^2}{S_2^2u^2t^2}(P_2 + \frac{S_2}{s_2}(ss_2+ut)(ut-2m^2s))(\ln\frac{S_2}{m^2} + 2\ln\frac{ut}{ss_2+ut}) - \frac{s_2^2}{S_2^2}\frac{8P_2}{u^2t^2} \\
&+ \frac{1}{2}\frac{s_2^2}{m^2S_2} - 1 + \varepsilon] \qquad\qquad \text{(C2)}
\end{aligned}$$

Note that parts of F_7^c, F_8^c and F_{11}^c proportional to $1-\varepsilon$ cancel out exactly in Eq. (4.5). The singular and finite parts of these integrals can be found in Appendix C of [12]; below we give the derivation of $\mathcal{O}(\varepsilon)$ terms.

We use the momentum parametrizations of Appendix A of [6] and, as in [12], we denote

$$F_n^{(k,l)} \equiv \int d\Omega_n (a + b\cos\theta_1)^{-k}(A + B\cos\theta_1 + C\sin\theta_1\cos\theta_2)^{-l} \qquad \text{(C3)}$$

where

$$\int d\Omega_n \equiv \int_0^\pi d\theta_1 \sin^{1-2\varepsilon}\theta_1 \int_0^\pi d\theta_2 \sin^{-2\varepsilon}\theta_2. \qquad \text{(C4)}$$

All the above integrals are proportional to $1/a^2 = 1/\omega_k^2\omega_2^2 \sim 1/s_2^2 \sim 1/(1-w)^2$; since the $2 \longrightarrow 3$ particle phase space is proportional to $(1-w)^{1-2\varepsilon}$, in view of Eq. (4.6), the terms of $\mathcal{O}(\varepsilon)$ give finite contributions proportional to $\delta(1-w)$.

Integral $F_7 \equiv \int d\Omega_n/(p_2 \cdot k)^2$:

This is of the type $\hat{I}_n^{(2,0)}$ of [12]. The result is

$$F_7 = -\frac{\pi}{a^2}\frac{1}{1+\varepsilon} = -\frac{\pi}{a^2}(1 - \varepsilon + \mathcal{O}(\varepsilon^2)) \qquad \text{(C5)}$$

Integral $F_8 \equiv \int d\Omega_n/(p_2 \cdot k)^2(p_1 \cdot p_4)$:

This is of the type $\hat{I}_n^{(2,1)}$ of [12], and determination of the $\mathcal{O}(\varepsilon)$ term proceeds as follows. First, defining

$$H \equiv A + B\cos\theta_1 + C\sin\theta_1\cos\theta_2, \tag{C6}$$

one can show the identity

$$\frac{1}{(1-\cos\theta_1)H} = \frac{1}{A+B}\left\{\frac{1}{1-\cos\theta_1} + \frac{B}{H} + \frac{C\sin\theta_1\cos\theta_2}{(1-\cos\theta_1)H}\right\} \tag{C7}$$

and by repeated application of it:

$$\begin{aligned}
&\frac{\sin\theta_1}{(1-\cos\theta_1)^2 H} = \\
&\quad \frac{1}{A+B}\{\frac{\sin\theta_1}{(1-\cos\theta_1)^2} + \frac{B}{A+B}[\frac{\sin\theta_1}{(1-\cos\theta_1)} + \frac{B\sin\theta_1}{H} - \frac{C(1+\cos\theta_1)\cos\theta_2}{H}] \\
&- \quad \frac{C\cos\theta_2}{A+B}[\frac{(1+\cos\theta_1)}{(1-\cos\theta_1)} + \frac{B(1+\cos\theta_1)}{H}] + \frac{C^2}{(A+B)^2}[\frac{\sin^3\theta_1\cos^2\theta_2}{(1-\cos\theta_1)^2} \\
&+ \quad \frac{B\sin\theta_1(1+\cos\theta_1)\cos^2\theta_2}{H} - \frac{C(1+\cos\theta_1)^2\cos^3\theta_2}{H}]\}
\end{aligned} \tag{C8}$$

Note that the fifth term vanishes due to the integration over θ_2. Also, terms with only H in the denominators are finite, consequently have no poles and cannot produce finite contributions from their $\mathcal{O}(\varepsilon)$ terms. Thus, we are left with the terms 1,2 and 7. After integrating them in n-dimensions, summing and keeping the relevant order ε terms, we arrive to the following result:

$$F_8^\varepsilon = \frac{\pi}{a^2(A+B)}\varepsilon \tag{C9}$$

Integral $F_{11} \equiv \int d\Omega_n/(p_2\cdot k)^2(p_1\cdot p_4)^2$:

Proceeding as before, the term of $\mathcal{O}(\varepsilon)$ is provided by

$$F_{11}^\varepsilon = \frac{\pi}{a^2(A+B)^2}\varepsilon \tag{C10}$$

Finally, we give the Brems integrals, F_i, $i = 12, ..., 21$, appearing in Eqs. (5.4) and (5.6). With

$$P_3 = 2m^2 s + u(s-s_2), \qquad Z = 4m^2 s(s+t) - s_2^2 t \tag{C11}$$

we have:

$$\begin{aligned}
F_{12} &= -\frac{1}{\bar{y}^2}[P_1(t\leftrightarrow u) + \frac{s}{2}P_3 F_{14}] \\
F_{13} &= -\frac{1}{\bar{y}^2}[\frac{2S_2}{sm^2}P_3 + P_1(t\leftrightarrow u)F_{14}]
\end{aligned}$$

$$
\begin{aligned}
F_{14} &= \frac{2S_2}{s_2\bar{y}}\ln\left(\frac{s_2(s-s_2)+2m^2s+s_2\bar{y}}{s_2(s-s_2)+2m^2s-s_2\bar{y}}\right) \\
F_{15}^s &= -\frac{2S_2}{s_2(s+t)}, \qquad F_{15}^c = 0 \\
F_{16}^s &= \frac{4S_2}{s_2su}, \quad F_{16}^c = -\frac{4S_2}{s_2su}[\ln\frac{S_2}{m^2}+\ln\frac{u^2}{(s+t)^2}] \\
F_{17}^s &= -\frac{8S_2(s+t)}{s_2s^2u^2}, \quad F_{17}^c = \frac{8S_2(s+t)}{s_2s^2u^2}[\ln\frac{S_2}{m^2}+\ln\frac{u^2}{(s+t)^2}-\frac{s_2P_3}{m^2s(s+t)}] \\
F_{18} &= \frac{4S_2}{s_2\sqrt{-tz}}\ln\left(\frac{Z-2m^2s(s+t)+s_2\sqrt{-tz}}{Z-2m^2s(s+t)-s_2\sqrt{-tz}}\right) \\
F_{19}^s &= -\frac{8S_2}{s_2^2s}, \quad F_{19}^c = \frac{8S_2}{s_2^2s}\ln\frac{sS_2}{ss_2+ut} \\
F_{20}^s &= \frac{S_2t}{(s+t)^2}, \quad F_{20}^c = \frac{P_1(t\leftrightarrow u)}{(s+t)^2} \\
F_{21}^s &= \frac{4S_2}{s_2st}, \quad F_{21}^c = -\frac{4S_2}{s_2st}[\ln\frac{S_2}{m^2}+\ln\frac{t^2}{(s+u)^2}]
\end{aligned}
\tag{C12}
$$

REFERENCES

[1] G. Baum et al, COMPASS Collaboration: CERN/SPLC 96-14 and 96-30.

[2] (a) R. Arnold, P. Bosted et al, SLAC-PROPOSAL-E156, 1997; (b) W.-D. Nowak, DESY 96-095; (c) A. de Roeck and T. Gehrmann, DESY-Proceedings-1998-1.

[3] M. Gluck and E. Reya, Z. Phys. **C39**, 569 (1988); B. Lampe and E. Reya, Phys. reports (in press). The latter is also a comprehensive review of polarized particle processes.

[4] M. Stratmann and W. Vogelsang, Z. Phys. **C74**, 641 (1997); A. Watson, *ibid* **C12**, 123 (1982).

[5] I. Bojak and M. Stratmanm: (a) Phys. Lett. **B433**, 411 (1998); (b) Nucl. Phys. **B540**, 345 (1999); Erratum: *ibid* **B569**, 694 (2000).

[6] B. Kamal, Z. Merebashvili and A.P. Contogouris, Phys. Rev. **D51**, 4808 (1995); Erratum: *ibid* **D55**, 3229 (1997).

[7] G. Jikia and A. Tkabladze, *ibid* **D54**, 2030 (1996).

[8] J. Smith and W.L. van Neerven, Nucl. Phys. **B374**, 36 (1992).

[9] P. Nason et al, *ibid* **B327**, 49 (1989).

[10] T. Muta, "Foundations of Quantum Chromodynamics" (Word Scientific, 1987)

[11] G. Passarino and M. Veltman, Nucl. Phys. **B160**, 151 (1979)

[12] W. Beenakker et al, Phys. Rev. **D40**, 54 (1989).

[13] R. Mertig and W. van Neerven, Z. Phys. **C70**, 637 (1996).

[14] W. Vogelsang, Phys. Rev. **D54**, 2023 (1996); Nucl. Phys. **B475**, 47 (1996).

[15] G.'t Hooft and M. Veltman, Nucl. Phys. **B44**, 189 (1972).

[16] B. Kamal, Phys. Rev. **D53**, 1142 (1996); *see also* A.P. Contogouris and Z. Merebashvili, *ibid* **D55**, 2718 (1997).

[17] A.P. Contogouris, S. Papadopoulos and B. Kamal, Phys. Lett. **B246**, 523, (1990).

[18] A. Hearn, REDUCE User' s Manual Version 3.6 (Rand Corporation, Santa Monica, CA, 1995).

[19] J. Vermaseren, FORM User' s Manual, NIKHEF-H, Amsterdam, 1990.

[20] T. Gehrmann and W. Stirling, Phys. Rev. **D53**, 6100 (1996).

[21] M. Gluck and W. Vogelsang, Z. Phys. **C55**, 353 (1992) and **C57**, 309 (1993); M. Gluck, M. Stratmann and W. Vogelsang, Phys. Lett. **B187**, 373 (1994).

[22] J. Hassan and D. Pilling, Nucl. Phys. **B187**, 563 (1981).

[23] H. Lai et al, Eur. Phys. J. **C12** (2000) 375.

[24] (a) Talk given by Z. Merebashvili at the International Workshop Spin 99, Prague, Czech Republic, 5-11 Sept. 1999, published in Czech. J. Phys, Vol. **50**, No. S1, 153

(2000); and hep-ph/9911506; (b) A.P. Contogouris, Z. Merebashvili and G. Grispos, Phys. Lett. **B482**, 93 (2000).

[25] B. Kamal and Z. Merebashvili, Phys. Rev. **D58**, 074005 (1998).

FIGURE CAPTIONS

Fig. 1. LO and loop graphs. In the loop graphs $p_1 \leftrightarrow p_2$ crossed ones are not shown. Note that graph (i), representing gluon, quark and ghost loop, does not contribute here.

Fig. 2. A) Gluon Brems graphs; $p_1 \leftrightarrow p_2$ crossed ones are not shown. B) Graphs of the subprocess $\gamma q \rightarrow Q\overline{Q}q$.

Fig. 3. Quantities related with the p_T distributions versus $x_T = 2p_T/\sqrt{S}$: Parts (a): Polarized differential cross sections; the LO (Born) ones are indicated by $*$. Parts (b): Asymmetries for sets A, B and C. 3I: $Q = c$, $\sqrt{S} = 10$ GeV. 3II: $Q = c$, $\sqrt{S} = 100$ GeV. 3III: $Q = b$, $\sqrt{S} = 100$ GeV.

Fig. 4. Quantities related with the rapidity Y distributions: Parts (a) and (b), as well as 4I, 4II and 4III as in Fig. 3.

Fig. 5. Quantities related with the integrated cross sections for $\vec{\gamma}\vec{p} \rightarrow Q + X$: (a) Factors $K = \Delta\sigma/\Delta\sigma_{LO}$ (b) Asymmetries.

Fig. 6. At c.m. energies $\sqrt{S} = 10$ and 100 GeV, for integrated cross sections and with solid lines for $\Delta\sigma$, dashed for σ and dotted for the asymmetry A_{LL}: a) The ratio R_m (see end of Sect. VI) with $m = m_c$; b) The fractional variation R_{sc} with the scale $\mu = M_f$ and with respect to $\mu = M_f = 3$ GeV. For both a) and b) the lines specified by $+$ refer to the corresponding quantities for $\sqrt{S} = 100$ GeV.

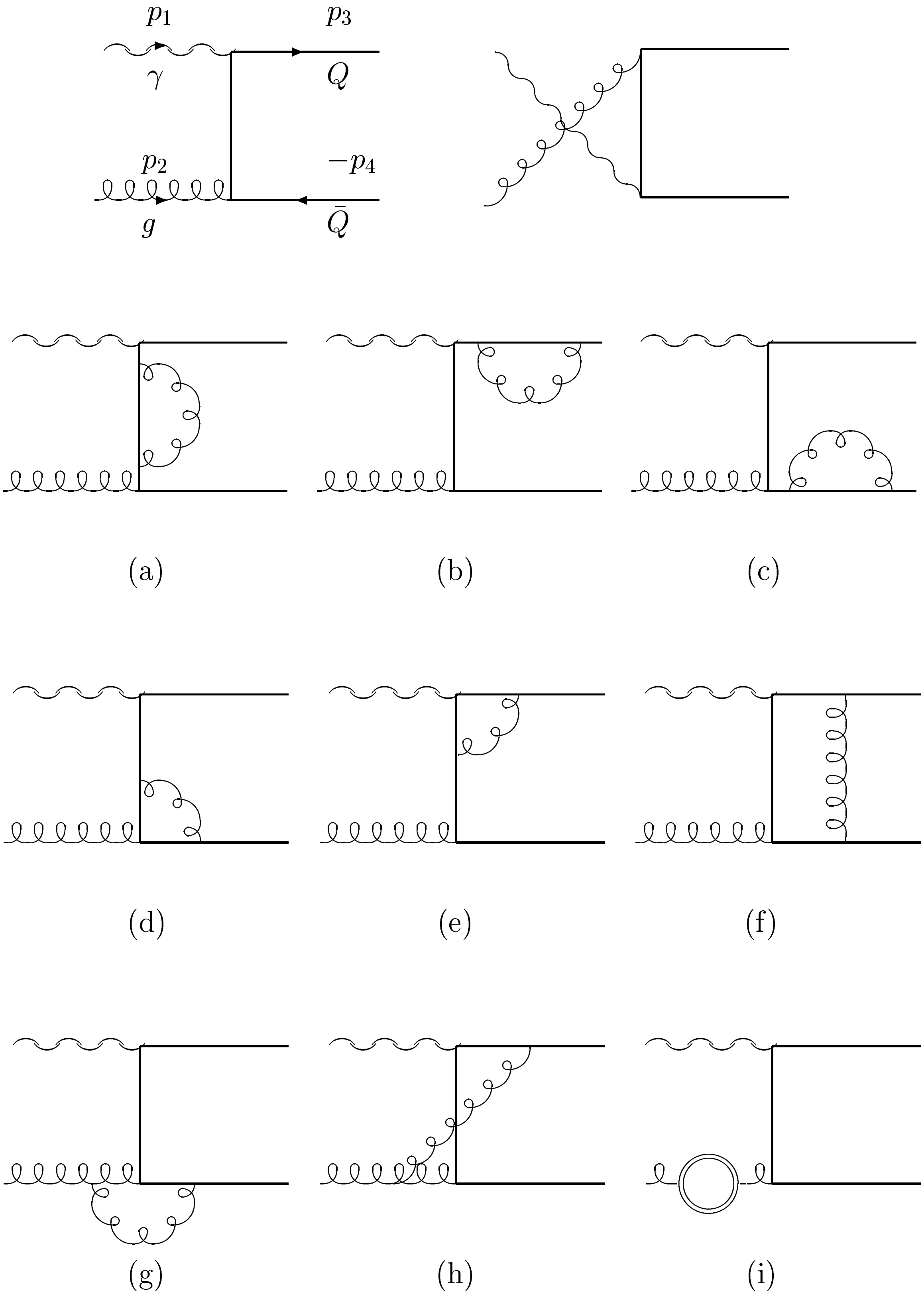

(a) (b) (c)

(d) (e) (f)

(g) (h) (i)

Fig. 1

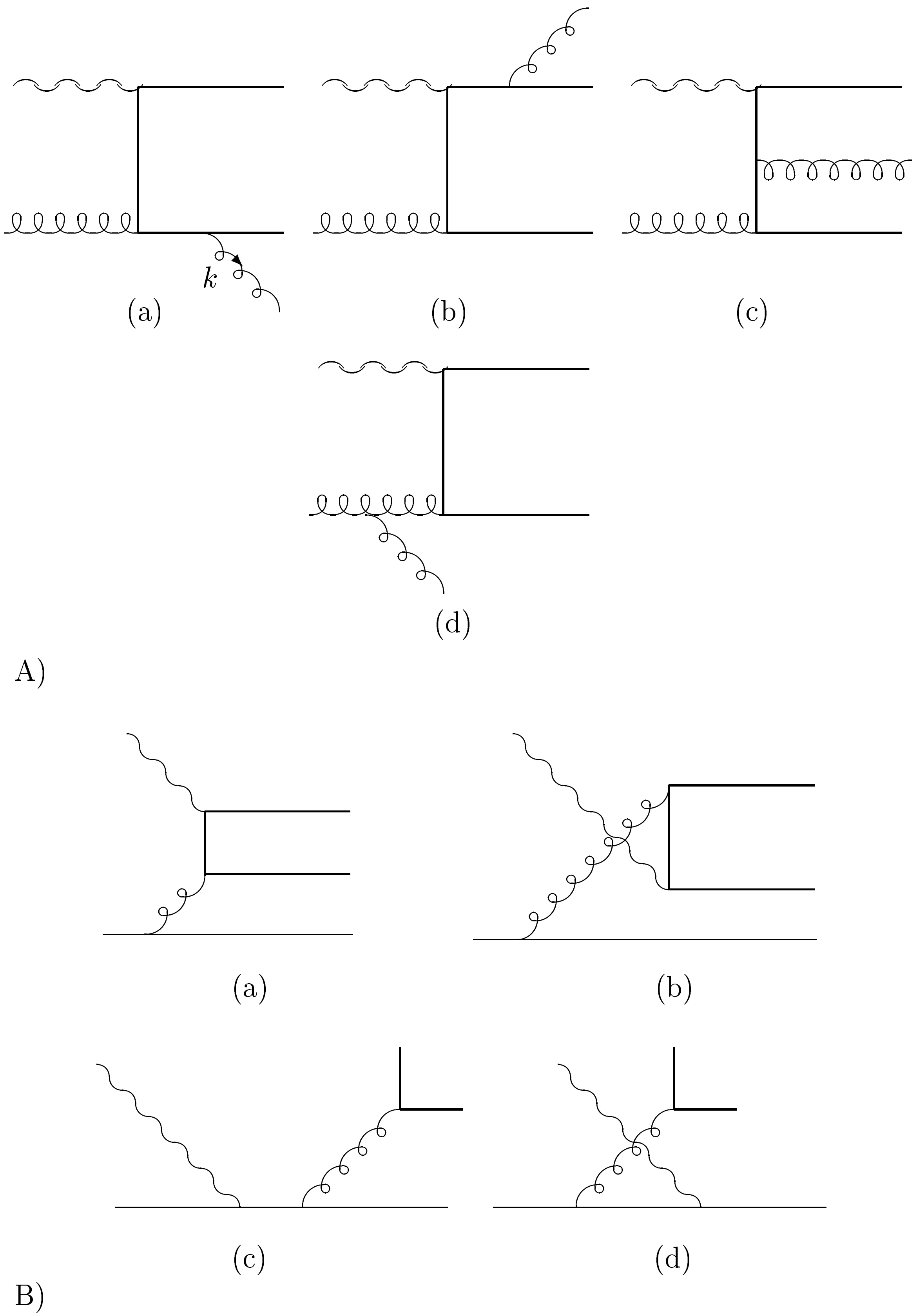

Fig. 2

c-quark
$\sqrt{S} = 10$ GeV

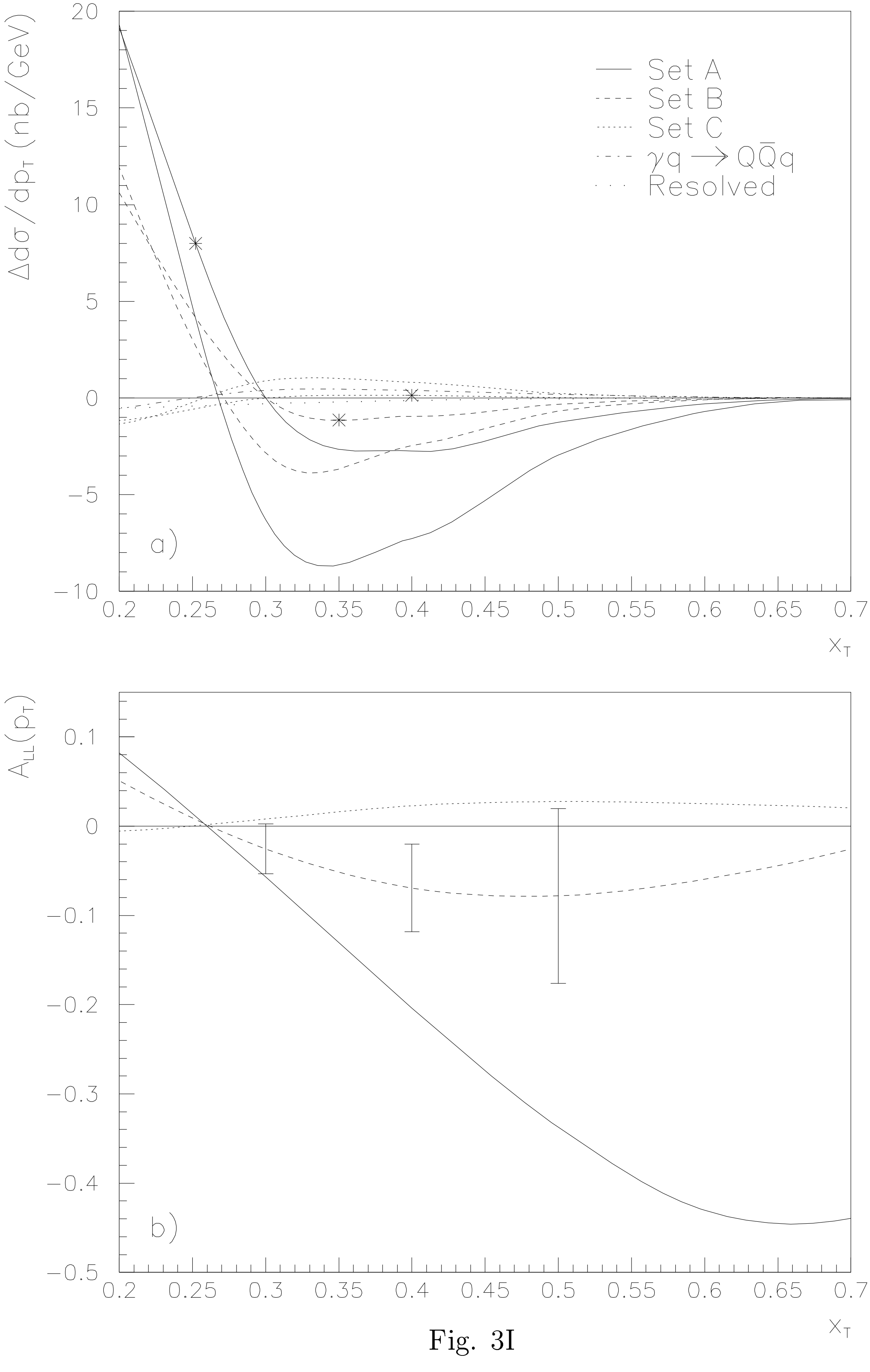

Fig. 3I

c-quark
$\sqrt{S} = 100$ GeV

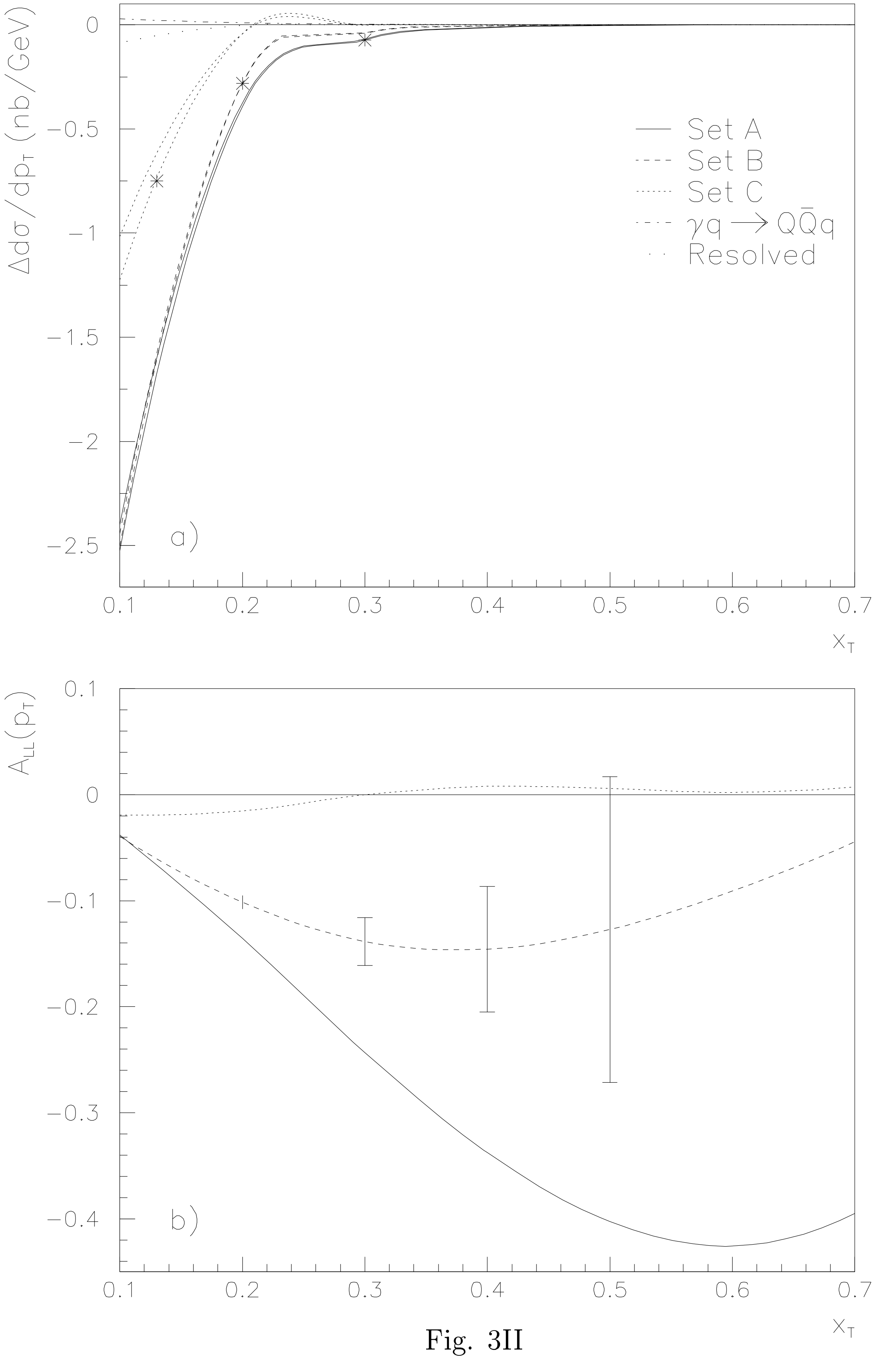

Fig. 3II

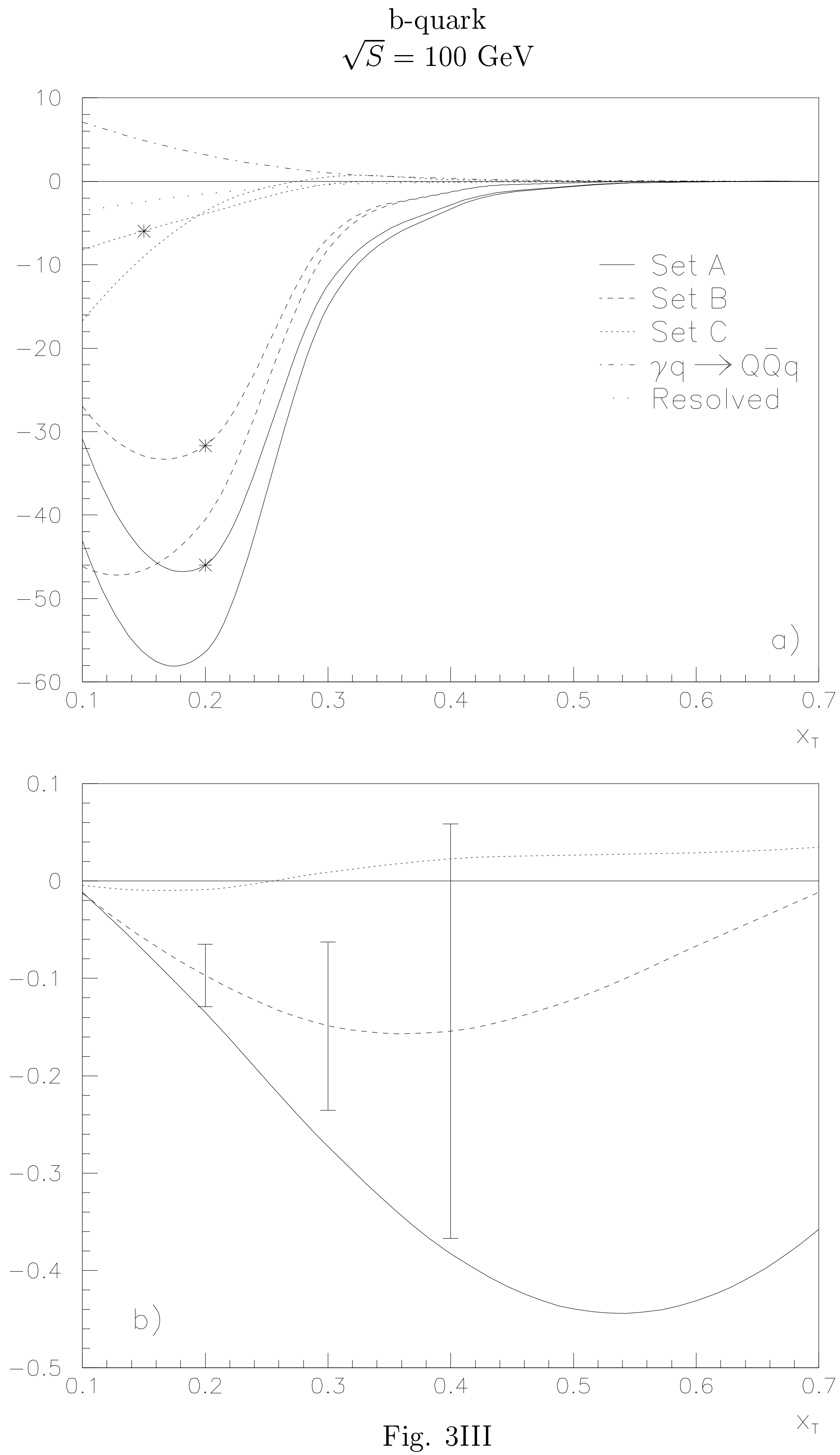
b-quark
$\sqrt{S} = 100$ GeV
$\Delta d\sigma/dp_T$ (pb/GeV)
10
0
−10
−20
−30
−40
−50
−60
Set A
Set B
Set C
$\gamma q \rightarrow Q\bar{Q}q$
Resolved
a)
0.1
0.2
0.3
0.4
0.5
0.6
0.7
x_T
$A_{LL}(p_T)$
0.1
0
−0.1
−0.2
−0.3
−0.4
−0.5
b)
0.1
0.2
0.3
0.4
0.5
0.6
0.7
x_T

Fig. 3III

c-quark
$\sqrt{S} = 10$ GeV

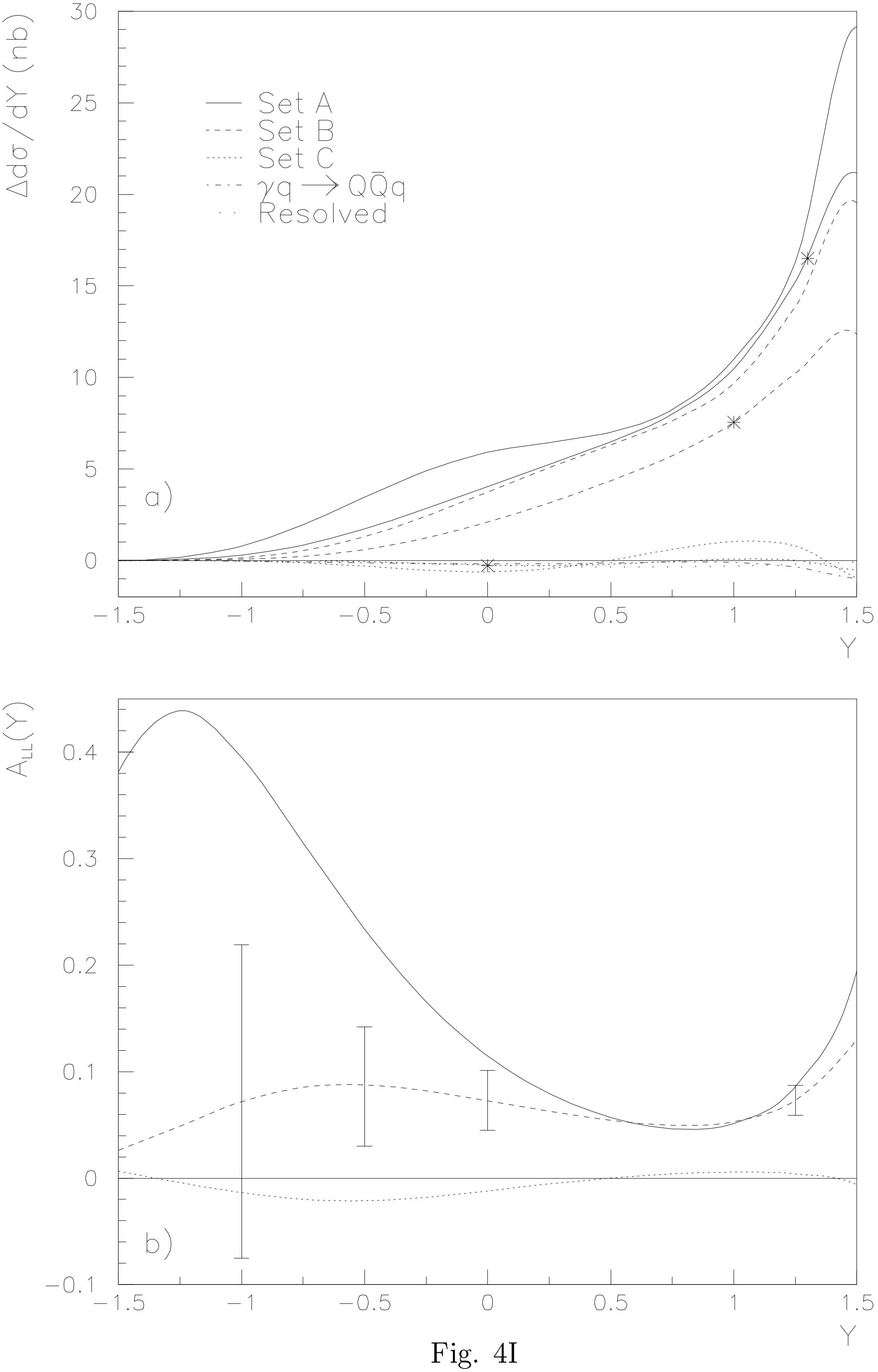

Fig. 4I

c-quark
$\sqrt{S} = 100$ GeV

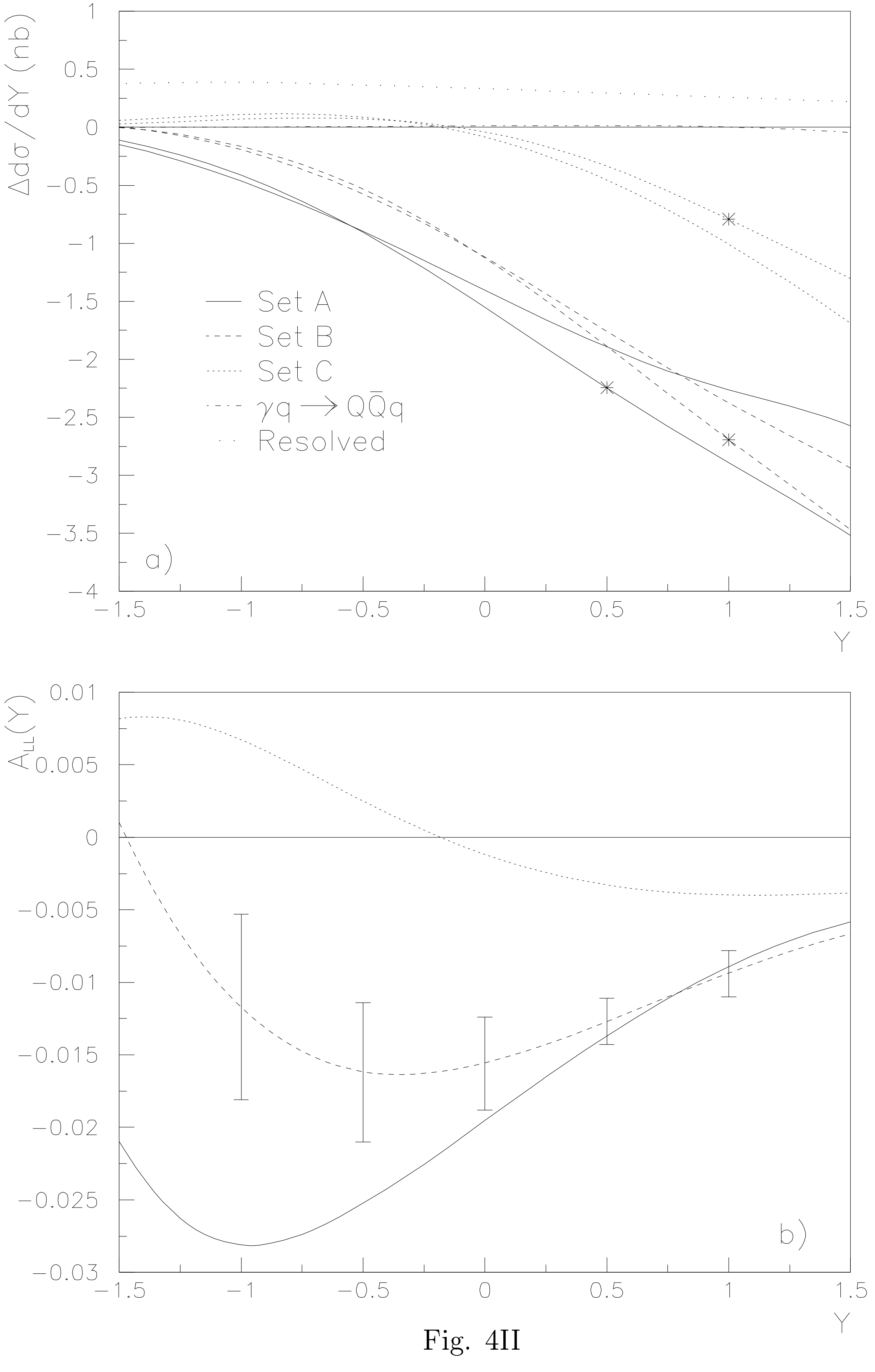

Fig. 4II

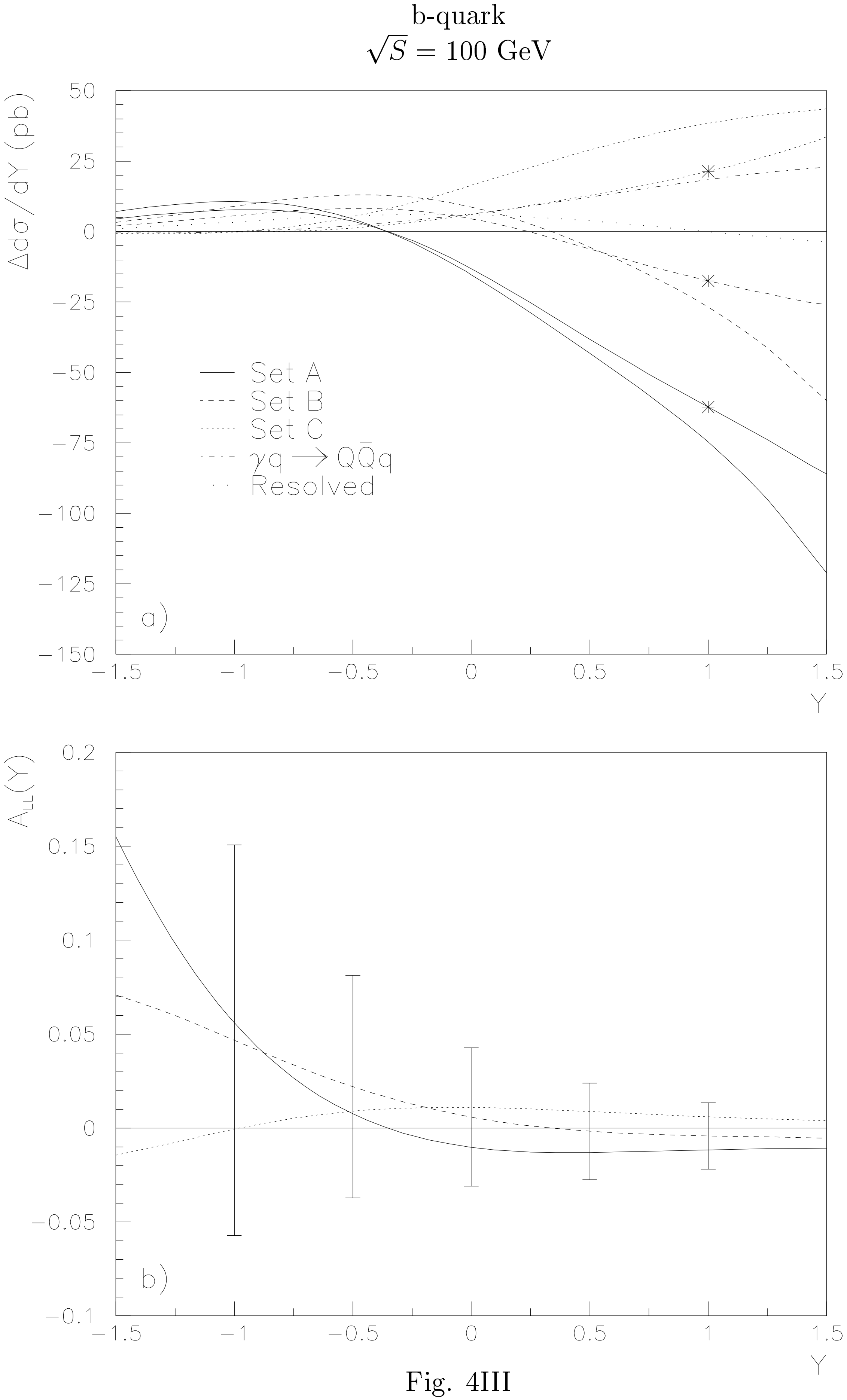
b-quark
$\sqrt{S} = 100$ GeV
$\Delta d\sigma/dY$ (pb)
50
25
0
−25
−50
−75
−100
−125
−150
Set A
Set B
Set C
$\gamma q \longrightarrow Q\bar{Q}q$
Resolved
a)
−1.5
−1
−0.5
0
0.5
1
1.5
Y
$A_{LL}(Y)$
0.2
0.15
0.1
0.05
0
−0.05
−0.1
b)
−1.5
−1
−0.5
0
0.5
1
1.5
Y

Fig. 4III

c-quark

$\sqrt{S} = 7 - 14$ GeV

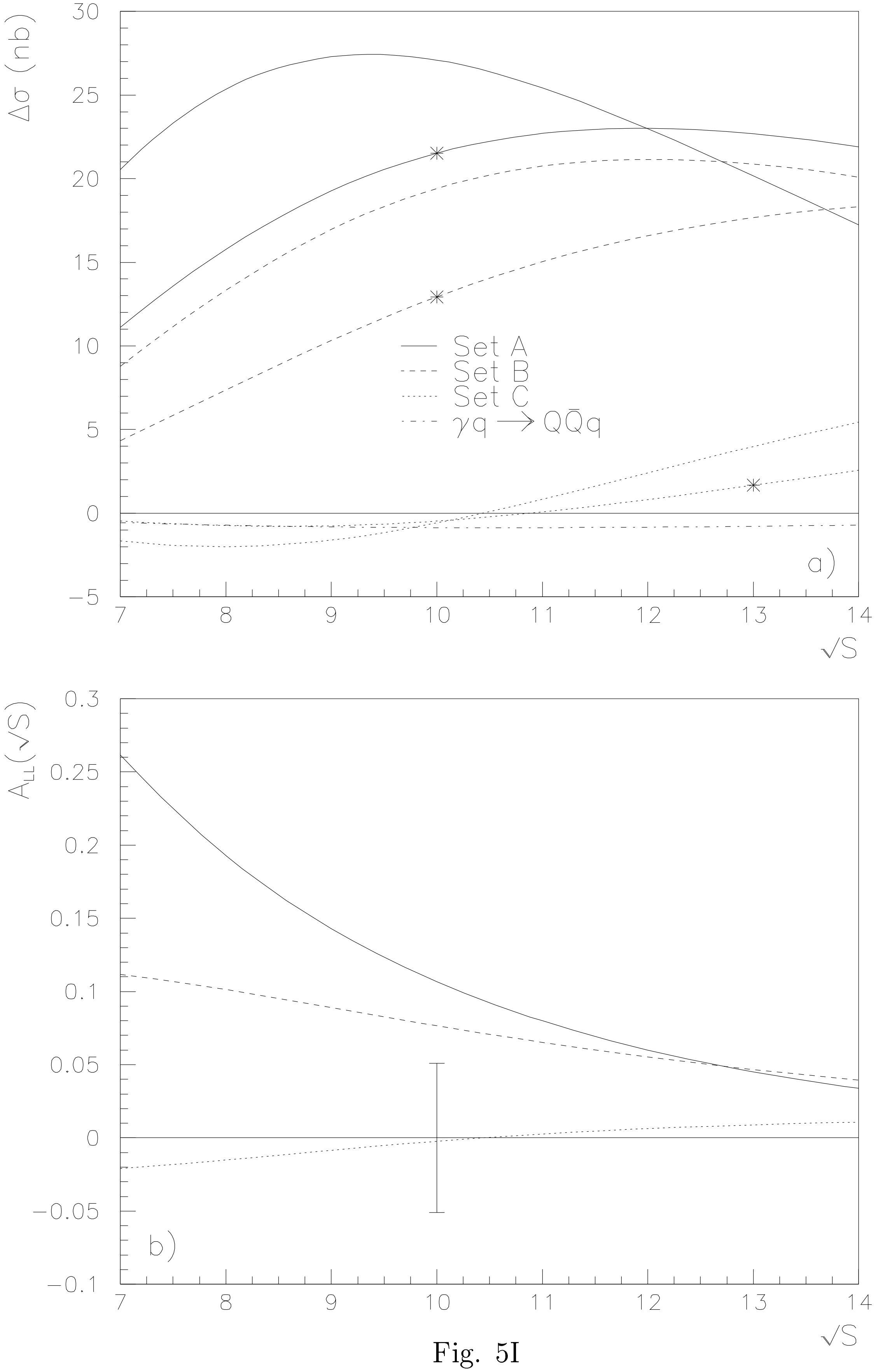

Fig. 5I

c-quark

$\sqrt{S} = 80 - 200$ GeV

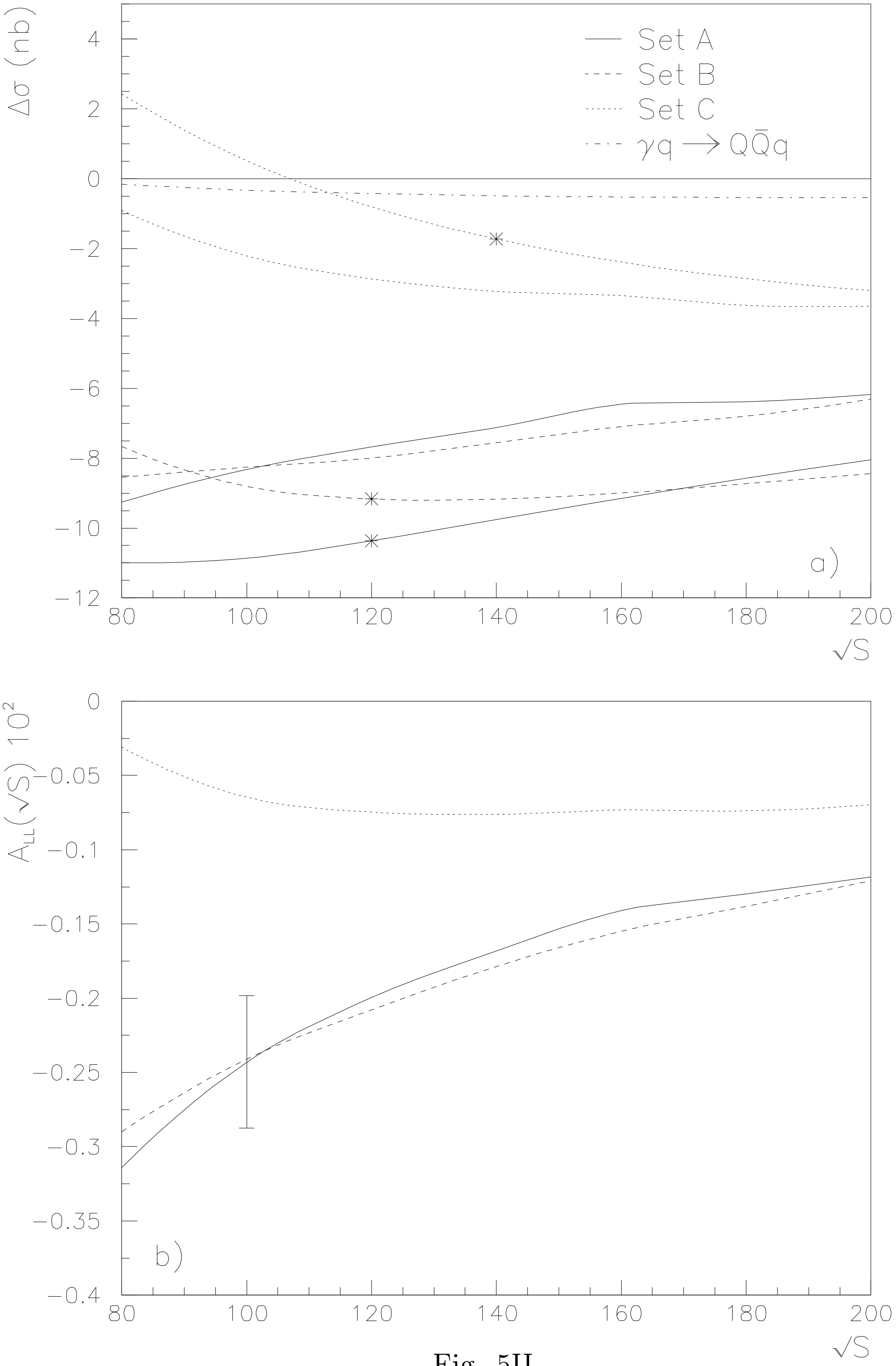

Fig. 5II

b-quark
$\sqrt{S} = 80 - 200$ GeV

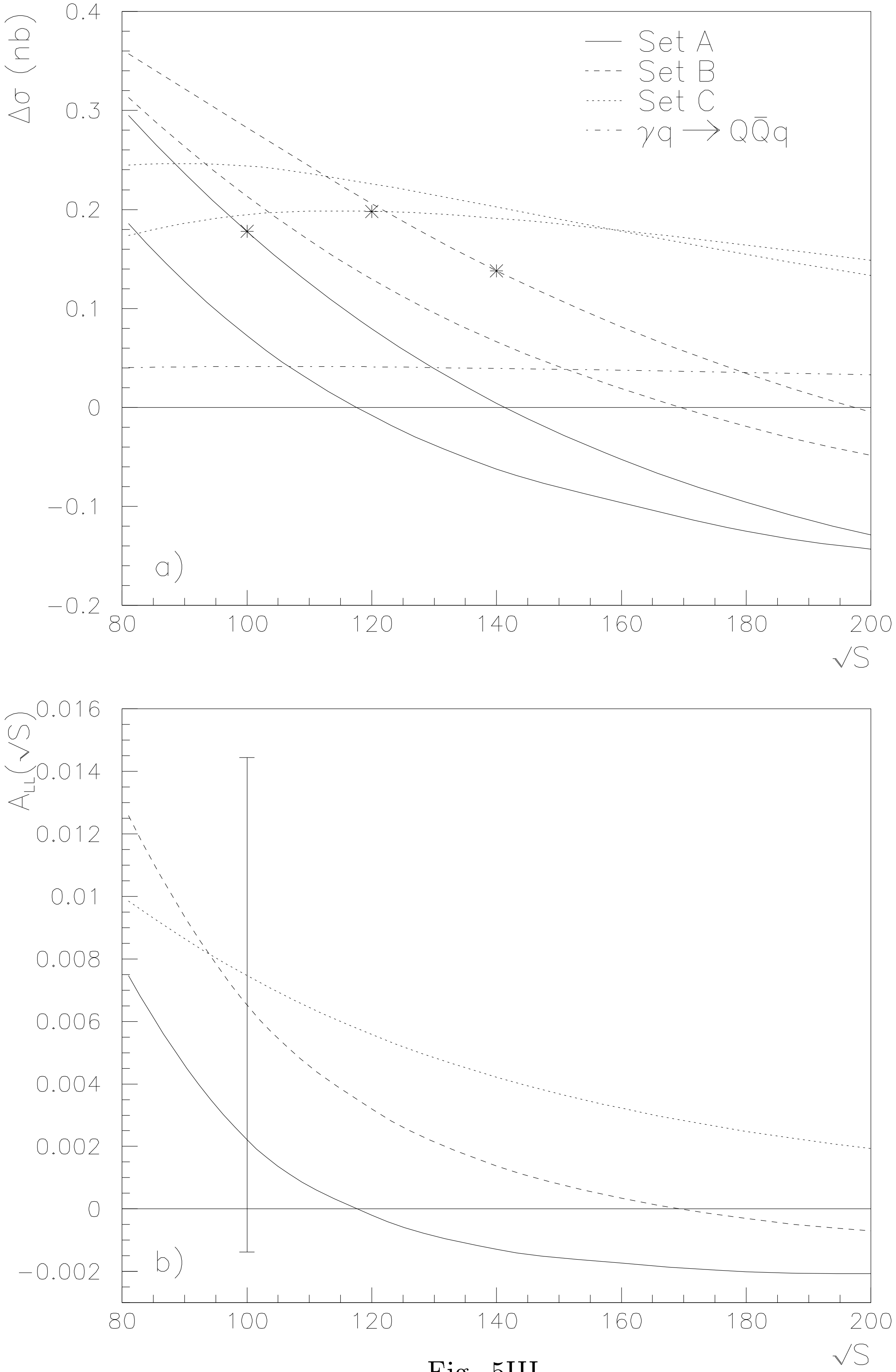

Fig. 5III

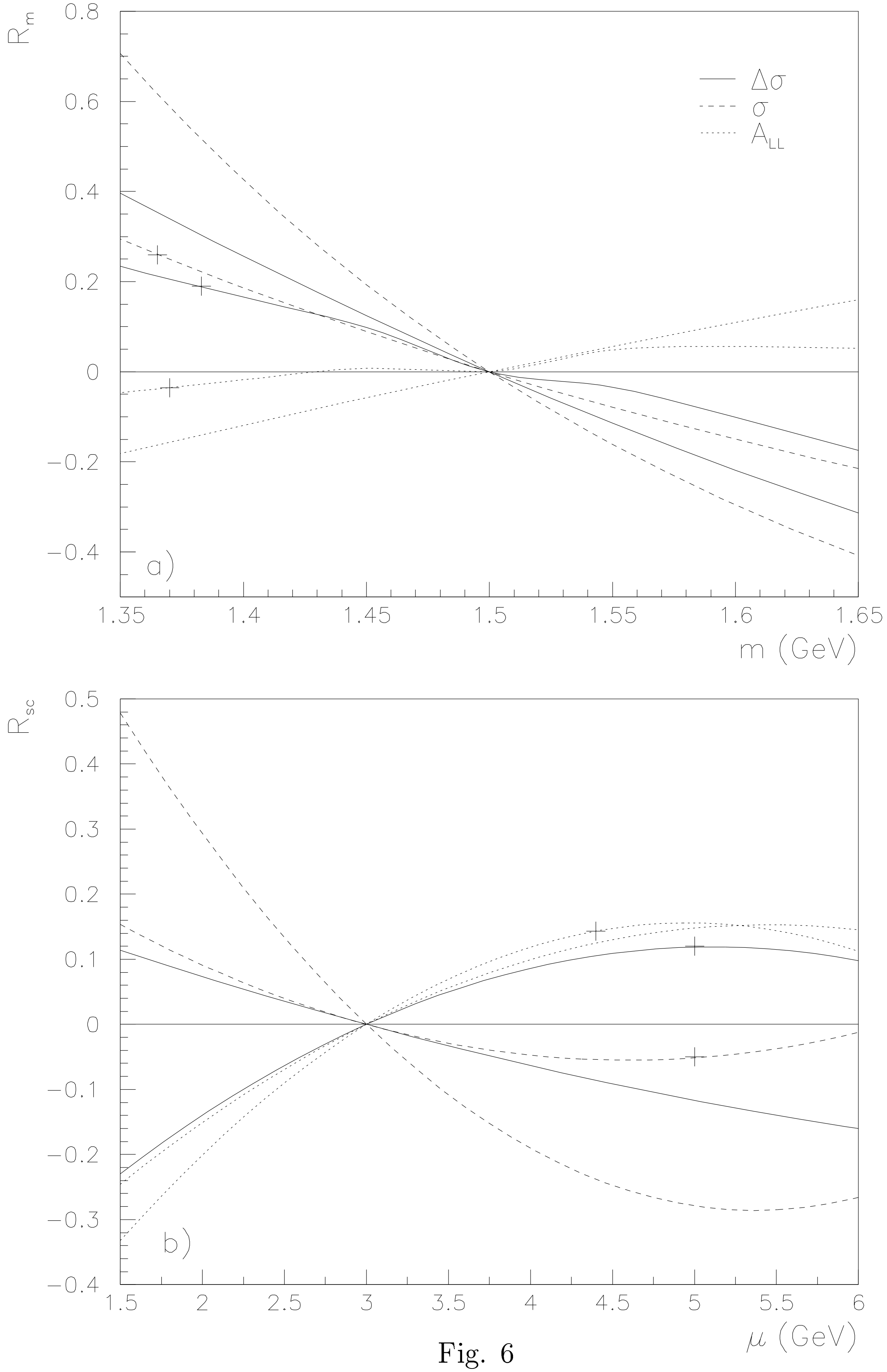
c-quark

$\sqrt{S} = 10$ and 100 GeV

Fig. 6